GC.SST.2013-2-605348

New Permanent MAGnets for Electric-Vehicle DRIVE Applications

MAG-DRIVE Project Final Report
01/10/2013 – 30/09/2016

Version No. 1

Contributions of all Workpackage and Task Leaders

2016/25/11

Distribution List:

- All partners of the MAG-DRIVE Consortium

Dissemination Level: CO Confidential, only for members of the consortium (including the Commission Services)

GC.SST.2013-2-605348

PROJECT FINAL REPORT

Grant Agreement number: 605348

Project acronym: MAG-DRIVE

Project title: New Permanent Magnets for Electric-Vehicle Drive Applications

Funding Scheme: FP7-SST-2013-RTD-1 - Small or medium-scale focused research project

Date of latest version of Annex I against which the assessment will be made: 19/01/2015

Period covered: from 01/10/2013 to 30/09/2016

Name, title and organisation of the scientific representative of the project's coordinator[1]:

Dr. Matej Komelj
Jozef Stefan Institute
Jamova 39
P.O. Box 3000
SI-1000 Ljubljana
Slovenia
Tel: +386 (1) 477 3308
Fax: +386 (125) 193 85
E-mail: matej.komelj@ijs.si

1 Usually the contact person of the coordinator as specified in Art. 8.1. of the Grant Agreement.

Project website[2] address: http://mag-drive-fp7.eu

2 The home page of the website should contain the generic European flag and the FP7 logo which are available in electronic format at the Europa website (logo of the European flag: http://europa.eu/abc/symbols/emblem/index_en.htm logo of the 7th FP: http://ec.europa.eu/research/fp7/index_en.cfm?pg=logos). The area of activity of the project should also be mentioned.

Declaration by the scientific representative of the project coordinator

I, as scientific representative of the coordinator of this project and in line with the obligations as stated in Article II.2.3 of the Grant Agreement declare that:

- The attached periodic report represents an accurate description of the work carried out in this project for this reporting period;
- The project (tick as appropriate) [3]:
  - ☒ has fully achieved its objectives and technical goals for the period;
  - ☐ has achieved most of its objectives and technical goals for the period with relatively minor deviations.
  - ☐ has failed to achieve critical objectives and/or is not at all on schedule.
- The public website, if applicable
  - ☒ is up to date
  - ☐ is not up to date
- All beneficiaries, in particular non-profit public bodies, secondary and higher education establishments, research organisations and SMEs, have declared to have verified their legal status. Any changes have been reported under section 2.2.1 (Project Management) in accordance with Article II.3.f of the Grant Agreement.

Name of scientific representative of the Coordinator: Matej Komelj

Date: 25/11/ 2016

For most of the projects, the signature of this declaration could be done directly via the IT reporting tool through an adapted IT mechanism and in that case, no signed paper form needs to be sent

3 If either of these boxes below is ticked, the report should reflect these and any remedial actions taken.

Table of Contents

FINAL REPORT

Publishable summary

Electro-motors may replace internal-combustion engines in the future vehicles. It is therefore of a vital importance to invest in development of electric drive. The working principle of any electric motor is based on a magnetic-torque-induced rotation, hence it is indispensable to provide a magnetic field, which can be produced either by coils or by permanent magnets. The formers make us possible to continuously control the field up to extremely high values by varying the applied electric current, whereas the magnets operate without any external power and can be shaped almost arbitrarily to fit into any motor design. Modern high-performance permanent magnets are made of alloys, which contain rare-earth elements. Due to the economical and political situation in the world the availability of these materials is limited. Particularly severe is the situation in the case of the so-called heavy-rare-earth elements, like dysprosium and terbium, which are added to the basic materials to enhance the performance of the magnets up to the level defined by the specifications of the electric motor. In order to reduce the manufacturing costs and even to prevent unexpected delays in production, it is necessary to invest in development of corresponding materials with a reduced amount of heavy-rare-earth elements, which is the main objective of the MAG-DRIVE project.

Further requirements for the material are related to the specific working conditions and environment: the temperatures of about 100 ^{0}C and corrosive atmosphere, in which the electric motors installed in vehicles operate. The next objective is therefore to make a magnet not just without using heavy-rare-earth elements and with the specified performance, but also with an ability to perform at such conditions. And the final goal is to integrate the magnets into an electric motor and/or an alternator with an improved and specially developed thermal management and power electronics, suitable as a power aggregate for electric vehicles.

The MAG-DRIVE consortium consisted of research partners: Jozef Stefan Institute (Slovenia), University of Birmingham (United Kingdom), Institute for Chemistry, Technology and Metallurgy (Serbia), Queen Mary University of London (United Kingdom), of a research and development company (SME) Kochanek Entwicklungsgesellschaft (Germany), of a magnet-producing company Magneti Ljubljana d.d. (Slovenia), and of a producer of components for automotive industry Valeo (France). The description of work was divided into nine work-packages (WPs). The development of material was covered in the work-packages WP3, WP4 and WP5. The activities within the WP7 and WP8 were devoted to the production and testing of magnets, and to the application of the magnets and the power-management electronics in electric motors and alternators. The WP6 was to provide the service, by means of magnetic and structural characterization, for the other research-and-development-oriented WPs. The WP1 was about the project management, whereas within the WP2 we defined the technical specification for the magnets and designed the power electronics in the basis of the requirements for the electric motors and alternators. The WP9 was devoted to the dissemination and exploitation.

The work-packages WP3, WP4 and WP5 had a common goal to produce a heavy-rare-earth-free powder of magnetic material with requested properties. The basic idea was to reduce the grain size and consequently took the advantage of the intrinsic-properties potential of the respective hard-magnetic phase in a much larger extent than in the case of the standard-processing techniques. Each of the three WPs followed a different route towards the goal. The final idea behind the activities in the WP3 was to produce the sufficiently fine powder by means of the wire-explosion experiment. The explosion was triggered by exposing a wire, made of material with the appropriate composition, to a short pulse of an extremely high electric current. Among the three routes, the wire-explosion route brought the most novelty to the production of permanent magnets. So, it is reasonable that we had to solve various problems, of which not all were predicted in the Description of Work. On the basis of extensive experiments, it was found that the reduction of the rare-earth oxides, i.e., samarium and neodymium oxide, which was the initially proposed procedure, was very low in a comparison with the reduction of transition-metal oxides. We successfully explained this phenomenon by means of phase diagrams and Gibbs free energies. It was concluded that an additional infiltration of the respective nano-particles would be required in order to obtain desired results. In agreement with the project officer it was therefore decided to proceed further just the wire-explosion-related activities on the Nd-based materials. Because of the additional experiments, it was also agreed to change the nature of the deliverables D3.1, D3.2 and D3.3 from the “prototype” to the “report”.

A more conventional technique was the method to achieve the goal in the work-package WP4. The idea was to apply the milling in a presence of light gases in order to get the powder with the particle size < 1 μm. The Task 4.1 was devoted to the survey of existing milling techniques as well as to making the decision for the most appropriate equipment. The Task 4.2 was to prepare the Nd-Fe-B powder with the particle size between 3 μm and 5 μm. It is, of course, also necessary to determine and to separate the particles with the desired size, which was the subject of the Task 4.3 in order to utilize the powder for the magnet production covered in the Task 4.4.

The most conventional method for the production of magnetic powder was included in the work-package WP5. The so-called HDDR process is based on the absorption and desorption of hydrogen accompanied with an optimum temperature regime. The result is a very fine magnetic powder, which can be compactified by means of the spark-plasma sintering. The particle size of the HDDR powder, and hence the magnetic properties, are very sensitive to the processing conditions, which are defined by the duration of different phases, the heating and cooling rates, and the corresponding temperature ranges. All these parameters were optimised on the basis of the results of the experiments related to the completed Task 5.1. The presence of any anisotropy is of the essential importance for the technologically-relevant magnetic properties. In order to get the maximum out of the HDDR powder, it is highly desired to align the particles. The Task 5.2 was to develop a procedure for pressing an aligned green compact, which was applied for the spark-plasma sintering. The underlying kinetics of this technique, which leads to a very dense material, is very complex. The related investigations, which improved the understanding, and consequently better results, were presented in the Task 5.3. The successful spark-plasma sintering (SPS) of the magnets was performed within the Task 5.4.

The work-package WP6 provided the magnetic and structural characterisation for the processing-oriented activities from the other work-packages as well as the corrosion tests on magnets. The main issues were the magnetic measurements and the electron microscopy. The relevant magnetic properties were determined from the measured hysteresis loop, which represents the magnetic response of a sample as a function of an external magnetic field. Roughly speaking, it is desired that the area surrounded by the hysteresis loop is as large as possible. The broadness of the loop is related to the quantity called coercivity, which is a measure of how difficult is to demagnetise a sample due to the influence of an external field. This is the most critical characteristic of a permanent magnet, which is in fact enhanced by the presence of undesired heavy-rare-earth elements. The magnetic measurements were covered in the Task 6.3. The hysteresis loops of powder samples were determined by applying the vibrating-sample magnetometer, whereas the permeameter was the appropriate measuring device for the magnets. Since both techniques require a certain calibration of the instruments, it was indispensable to compare the results obtained for a magnet and for a corresponding powder, which was carried out. However, an eventual discrepancy might be, to some extent, ascribed also to the preparation techniques, which connect the two states of the same magnetic material. The scanning-electron microscopy, which was covered in the Task 6.1, is arguably the most important characterisation method in materials science. The resulting images represent the microstructure, i.e., the information about the distribution of different phases, grain size, and morphology. Practically any material produced in any of the processing work-packages was characterised by means of this technique. For, example, it was very useful for setting up the optimal parameters for the HHDR process during the investigations related to the Task 5.1 because it readily offered the information about an eventual undesired grain growth or about the existence of undesired phases, like the α-Fe. In order to analyse the chemical composition of a particular phase we applied either the energy-dispersive X-ray spectroscopy (EDXS) or electron-energy loss spectroscopy (EELS), which were both covered in the Task 6.2. This included also other techniques, for example, transmission-electron microscopy, which made us possible to analyse the structure on atomistic level, or laser confocal microscopy for 3D imaging, which was important for controlling porosity in green compacts for spark-plasma sintering. Part of the work-package WP6 was also the Task 6.4, which was strongly related to the activities from the work-package WP5, providing the quantitative data about the particle size and surface of the milled powder, and the Task 6.5 devoted to the corrosion tests. Basically, in these tests, the corrosion resistivity was supposed to be disproportional to the loss of the magnet mass upon exposing the samples to elevated temperatures and high humidity for a certain amount of time. The experiments revealed the importance of an appropriate coatings to prevent the magnets from decaying. The relevant results of all measurements in the WP6 were presented in deliverables D6.1, D6.2, D6.3, D6.4, D6.5, D6.7 and D6.8.

The work-package WP7 led to the production of magnets by applying the spark-plasma sintering (SPS) and innovative flash-spark-plasma sintering (FSPS) techniques covered by the Tasks 7.1 and 7.2. In the Task 7.3 we chose the sets of the best and the most compatible magnets, whereas the Tasks 7.4 and 7.5 were to optimize the power electronics for the electric motors.

Within the work-package WP8 we successfully tested the produced magnets in terms of their magnetic and physical properties as well as of their resistance upon environmental conditions. The final consortium meeting we held was also a part of the WP8. We critically assessed the results, which were achieved during the course of the project, and discussed the possibilities for further joint activities.

The work-package WP9 covered the dissemination and exploitation activities in addition to the preparation of the reports, which were all submitted to the EC.

Core of the final report: Project objectives, work progress and achievements, project management

1 Project objectives

Objectives: The objectives were valid for the entire duration of the project with differing intensity.

A: The focus of the overall objectives was targeted towards:

developing high-coercivity hard-magnetic materials without heavy-rare-earth elements like dysprosium or terbium by dramatically reducing the grain size to below 1 μm using three novel processing routes
using the developed materials to produce demonstrator magnets applicable for electric-vehicle motors
optimisation and the thermal management of the power electronics and rotors in electric motors
efficient project coordination, quality of all activities, timely delivery of reports and deliverables, effective and on-time communication between the project consortium and European commission, preparation of rolling 6-monthly Action plan

B: Objectives related to short-term activities and progress:

to provide industrial specifications and the technical requirements for the magnet demonstrator and the new electric motor, which was completely achieved in the WP2
to build up nanocrystalline hard-magnetic materials in principles of the wire-explosion experiment, which was completely achieved in the WP3.
to provide magnetic powder of particle size in the order of magnitude of 1 μm by means of “light-gas” milling procedures, which was completely achieved in the WP4.
to produce HDDR-processed Nd-Fe-B anisotropic magnetic powders with the grain sizes in the sub-micron region, which was completely achieved in the WP5.
to constantly provide a characterisation of structural and magnetic properties of the materials, produced in WP's 3,4 and 5 by means of electron microscopy and state-of-the-art magnetic measurements, which was completely achieved in the WP6.
to prepare the magnet-processing equipment, and to perform the pressing, sintering and magnetization of samples, which was completely achieved in the WP7.
to define and to report on the testing procedures, and to report on the structural, magnetic and corrosion-resistance tests, which was completely achieved in the WP 8.
to maintain external project communication, and to guarantee the impact of the project through the creation of a comprehensive exploitation plan, which was completely achieved in the WP9.

2 Work progress and achievements

WP 1: Project Management (M1 - M36)

WP Leader: Matej Komelj(JSI)

Summary of Results

The MAG-DRIVE management was lead by JSI. The main goals were to:

- Ensure efficient project coordination, progress monitoring, budget and financial control
- Ensure the quality of all activities and the timely delivery of reports and deliverables

- Ensure effective and on-time communication between the project consortium and the European Commission through the REA

- Prepare the rolling 6-monthly Action Plan

There were no deviations from the objectives and tasks given in Annex I.

Details for each Task

2.1 Task 1.1: Project management (M1 – M36)

The coordinator was responsible for the day-to-day coordination of the project, project planning, progress, reports, deliverables, cost statements and budgetary overviews, contract negotiations and all financial and legal , issues, contingency plans and risk management, notes, minutes, and other materials, managing any necessary changes to plans or contracts, ensuring that the project proceeds on time and on budget , and represents the interface between the consortium and the REA. JSI prepared the Consortium Agreement, which was approved by all partners.

There were seven meetings:

11.10. 2013 *Brussels*
First meeting (11 participants)

04. 04. 2014 *Brussels*
M6 meeting (11 participants)

17. 10. 2014 *Brussels*
M12 meeting (14 participants)

05. 02. 2015 *London*
M18 meeting (15 participants)

17.09. 2015 *Paris*
M24 meeting (14 participants)

21.04. 2016 *Belgrade*
M30 meeting (15 participants)

21.09. 2016 *Neustadt*
M36 meeting (13 participants)

From all meetings, agendas, presentations, minutes and photos are available for download on the protected part of the MAG-DRIVE web page.

On 04. 02. 2015 an amendment to the grant agreement was issued. It specifies the change of the name and address of the project coordinator in Article 8.1 of the grant agreement as:

Dr. Matej Komelj

INSTITUT JOZEF STEFAN

Department of Nanostructured materials

Jamova 39

LJUBLJANA 1000

SLOVENIA

and in Article 8.3 as: matej.komelj@ijs.si

Accordingly also the Part A and B of the Annex I were modified. The valid version is dated 19. 01. 2015

On the basis of the first research activities within WP3 it was decided that the nature of the deliverables D3.1 D3.2 and D3.3 was changed from the prototype to the report. For the same reason the deliverable D3.4 was postponed from M18 to M24. All the changes were approved by the project officer, and they did not have any impact on the realization of the project objectives.

Dr. David Brown, a member of the External advisory board, was contacted monthly in the first 18 months for advices related to activities within WP3.

2.2 Task 1.2: Preparation of 6-monthly Action Plan (M1 – M30)

A rolling Action Plan was prepared every six months. It included details about the activities for the next six months, broken down to a weekly schedule of sample movements, tests, results, and information flow between partners.

2.3 Task 1.3: Creation and maintenance of project website (M1 – M36)

The MAG-DRIVE website with the url address http://mag-drive-fp7.eu was created. The website features a public-accessibly area and an intranet section. The intranet section can be left via a logout function, for safety reasons. The website was regularly maintained and frequently updated.

WP 2: Technical Requirements (M1 - M8)

WP Leader: Jean-Marc Dubus (VALEO)

Summary of Results

All the activities within the WP 2 were finished in the first eight months. According to the plan we performed a detailed survey of industrial specifications and technical requirements for the demonstrator and the new electric motor. It was found that there were two competitive technologies in terms of performance and price, both with some advantages and disadvantages. Available products from the leading manufacturers were analysed in detail. The problem of cooling was addressed not just by designing but already by providing some prototypes for the required electronic circuits. Finally, we obtained the information about the currently available permanent magnets to be build in the electric motors.

There were no deviations from the objectives and task given in Annex I.

Details for each Task

2.1 Task 2.1: Benchmarking electric motors (M1 – M3)

Electrical vehicles can be configured in a number of different ways. Based on various considerations, for example, required output power and the available space, a choice is made between integrated starter generators (ISGs) and belt-drive starter generators (BSGs):

- The main advantage of the ISG machine is that it can be used for ZEV driving and to maximize the regenerative braking power, as the thermal engine could be disconnect through a clutch mechanism.The main drawback of the ISG machine was the mechanical integration in between the combustion engine and the gearbox, which increases the operating costs.The comparative analysis of the competitor machines focused on the following: power density, efficiency, high torque at low speed in E-drive, cooling system, use of raw materials (in particular the use of RE), machine technology

A graph showing the various areas that these motors occupy in the areas of Mild Hybrid and Full Hybrid are shown below. We tested machines from the following companies:

Honda

Porsche

Mercedes

Cadillac

Lexus

Toyota

Kia

These motors where purchased on the open market from the OEMs.

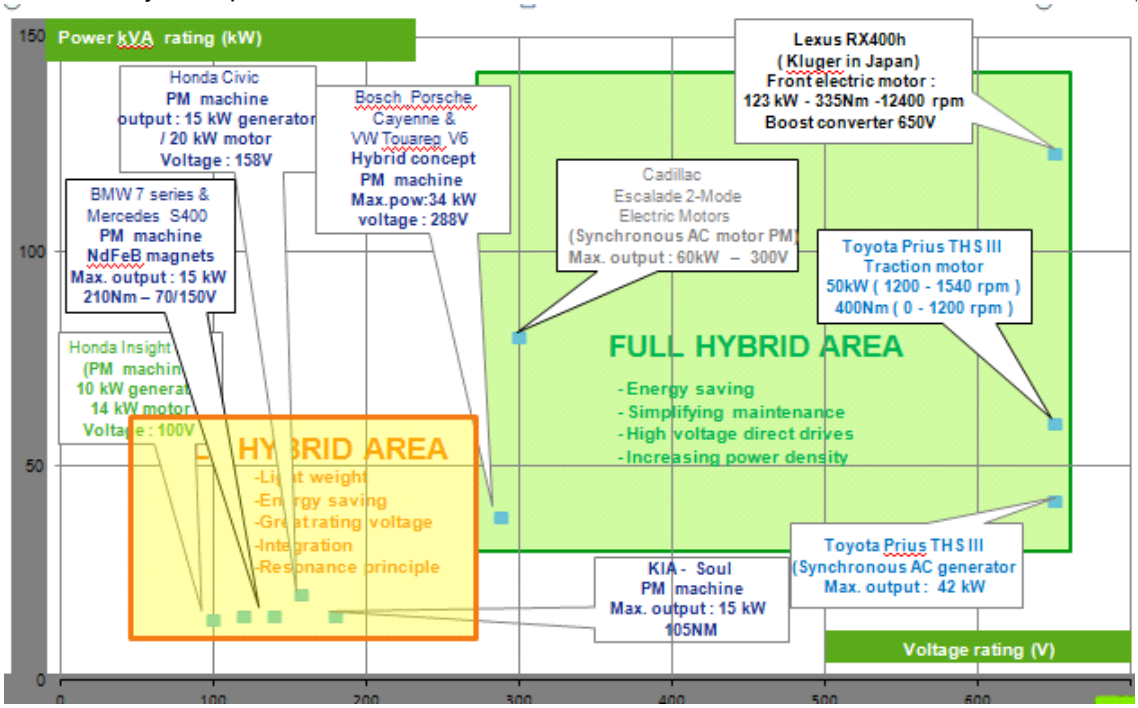

Graph showing the power rating for various electric motors tested as part of the MAG-DRIVE project. The bottom-left-hand side of the graph shows the low power outputs of electrical motors tested in the Mild Hybrid area. The top-right-hand side of the graph shows motors with very high power outputs, including the 123 kW motor from the Lexus RX400h.

In the next figure we can see the results of the testing on some electrical motors that fall into the following categories:

Mild hybrid electrical vehicle (HEV)

Mild & Full HEV

Full Hybrid with Plug-in

The motors were tested as received and then stripped and cut away for imaging and other tests on the materials in the motors.

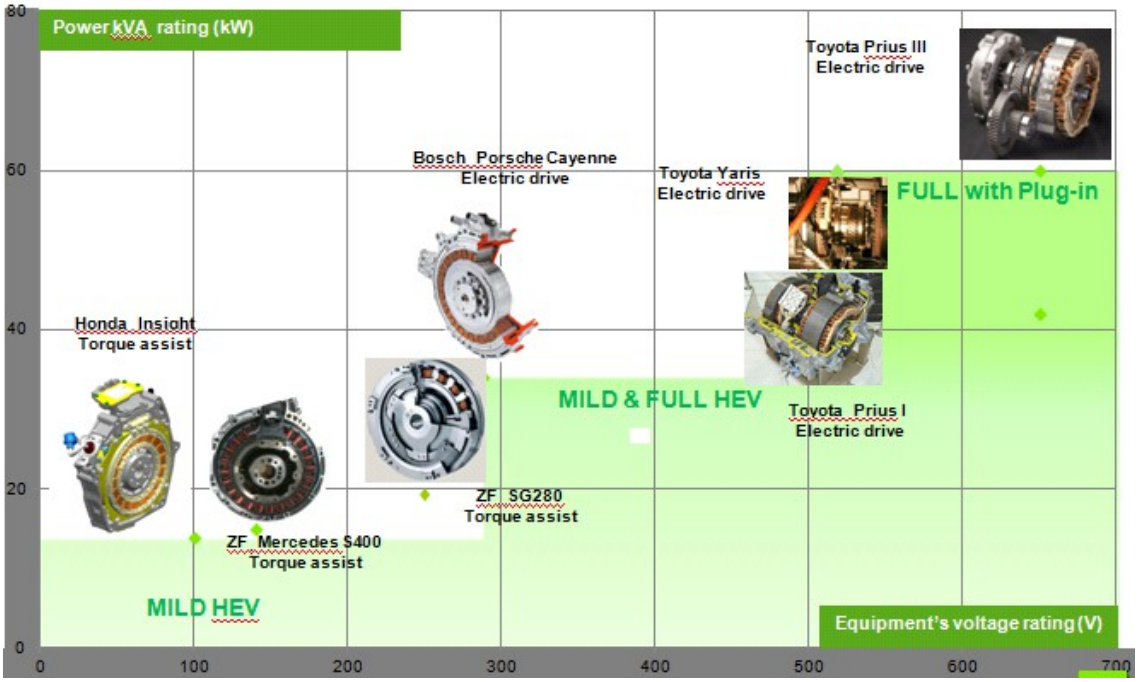

Power rating graph showing some of the motors that were tested as part of the MAG-DRIVE investigation.

Detailed tests were carried out on motors from:

Porsche (manufactured by Bosch)

Toyota

Renault (manufactured by Continental)

VW (manufactured by ZF Sachs)

The motors ranged in terms of the power output from 20 kW to 45 kW. Sizes were in the range 200 to 300 mm. Special attention was given to the position and orientation of the magnets. The Toyota motors all used embedded magnets with a “V” configuration. The German motors favoured a surface positioning of the magnets. It is important to note that the Continental motor, produced for the Renault Kangoo contains no magnets. Of course this motor has a large weight penalty as a result.

	Bosch Porsche Cayenne	Toyota Prius III Generator	Toyota Yaris Traction motor	Toyota Yaris Generator	Continental Renault Kangoo	ZF Sachs SG280 VW Jetta Hybrid
Vehicle and supply						
Motor peak power voltage	34 kW @288 VDC	42 kW @650 VDC	45 kW @520VDC	20 kW @520VDC	44 kW @220 VDC	20 kW @250VDC
Motor peak torque	300 Nm	~	169 Nm	~	226 Nm	265 Nm
Ext diameter (without bracket)	300 mm	246 mm	201 mm	201 mm	210 mm	280 mm
Iron thickness	56 mm	27 mm	54 mm	24.25 mm	170.5 mm	32 mm
Magnet disposition	Surface magnet	Embedded magnet with "V" configuration	Embedded magnet with "V" configuration	Embedded magnet with "V" configuration	Without magnet Exciting coil	Surface magnet
Total weight	**32kg**	**8.5+4.0 = 12.5kg**	**11.6 + 5.9 = 17.5kg**	**6.84 + 3.15 = 10.0kg**	**25.5 + 20 = 45.5kg**	**6.9 + 8.1 = 15.0kg**

Investigated electrical motors for the MAG-DRIVE project. All the motors in the figure are based on the use of permanent magnets, except for the Continental-built motor for the Renault Kangoo.

The next stage was to look more closely at the rotors of these various electrical machines. The details of the MAG-DRIVE investigation can be found in the figure.

The key points to notice here are the numbers of magnets, i.e., from 16 to 120, the dimensions of the magnets, and the total weight of the magnets. The final performance figure is also very important as it shows the power output per gram of RE permanent magnet used in the motor.

ROTOR	Bosch Porsche Cayenne	Toyota Prius III Generator	Toyota Yaris Traction motor	Toyota Yaris Generator	Continental Renault Kangoo	ZF Sachs SG280 VW Jetta Hybrid
Pole pairs	12	4	4	4	4	16
Inner diameter (mm)	195	90	50.48	95.3	45	252.3
Outer diameter (mm)	225	151	146.14	146.14	133	280
Nb magnet	24 x 5 = 120	16 x 4 = 64	16	16	"0"	32
Magnet dimension (mm)	22 x 10 x 4	21.06 x 6.35 x 6.69	52 x 14 x 7	23 x 20 x 5	Without	32 x 20 x 4
Type flux	Surface	Concentric flux	Concentric flux	Concentric flux	8 Exciting coils	Surface
Mag-mode pose	5 elements offset	"V" configuration	"V" configuration	"V" configuration	117 turns/coil	Glue on the surface
Magnet weight (g)	792	448	611	276	Not applicable	675
Peak power (kW)	34 - @288VDC	42 - @650VDC	45 - @520VDC	20 - @520VDC	44 - @220VDC	20 - @250VDC
Perfo.estimate (W/g)	42,9				Not applicable	30

Detailed breakdown of the rotor in terms of the magnets, dimensions and performance.

The next table in figure describes the strong points, benefits and drawbacks to the various motors described above.

ROTOR	Bosch Porsche Cayenne	ToyotaPrius III Generator	Toyota Yaris Traction motor	Toyota Yaris Generator	Continental Renault Kangoo	ZF Sachs SG280 VW Jetta Hybrid
Mag. performance estimated Φ - total Flux per pole at no-load condition F - total MMF per pole S - magnet section l - magnet thickness	Surface	Concentric flux	Concentric	Concentric	Winding Excitation	Surface
Strong points	1 – Pole is consisted by 5 elements offset which are inserted in the home to decrease the harmonic 2 - Hollow plate for shaft coupling to minimize the stray flux flowed in the shaft	1 - Form of magnet's home optimized patent 20120223607A1 2-4 small magnets superimposed and glued into magnet home. 3 - Bigger hollow shaft diameter	1 – Form of magnet's home & Opening stack optimized; As TOYOTA Prius reference 2- Hollow shafts more than TOYOTA Prius. 3- Decreased magnet weight 4- Any balance drilling point found, even if in question		1_ Excitation coil 2_ Good protection on all rotor's surface to hold mechanical & thermal shock Patent 202012003643 U1 202012003643 202012002024 3_ Declined pole 4_ Positing censor no need adjust	1 - External rotor is composed of straight magnets, which are glued in the internal diameter of a thin ferro-magnetic ring
Benefits	+ Harmonic reduced + Small leakage flux flowed in the shaft	+ Decrease Eddy loss + MMF performance increased	+ Easy to produce + Magnet performance more than TOYOTA Prius + Decreased more inertia also		+ "0" magnet & Magnetic fields variable in different work condition + Harmonic reduced + Mechanical & thermal strong	+ Easy produce + No magnetic leaking in the rotor ring
Drawbacks	- Increased number of magnets due to circumference	- Increased number of magnets and need of glue	- Necessity to glue around magnets		- Not easy to produce, expensive , heavy & cumbersome	- Many of hand work - Increase magnet used on big circumference

Rotor performance, strong points, benefits, and drawbacks. Relevant patents with respect to the MAG-DRIVE project are also mentioned in the figure.

The best power density is achieved by the Toyota Yaris electrical machine. This is mainly due to the use of high-grade Nd-Fe-B magnets and a high stator-filling ratio of 2,5kW/kg of raw material. The lowest power density was measured for the Renault Kangoo motor due to the wound rotor: 1kW/kg.

- The main advantages of belt-driven machines are that they fit in the place of standard alternator, they are cheap and could achieved 85% of the CO2 reduction at about half of the price of an ISG system. However, the main drawback is that they are not as efficient as the ISG architecture in regenerative-braking mode. In the comparative analysis of our competitors, we focused on the following: power density, efficiency, high torque at low speed in E-drive, cooling system, use of raw materials (in particular rare earths), machine technology

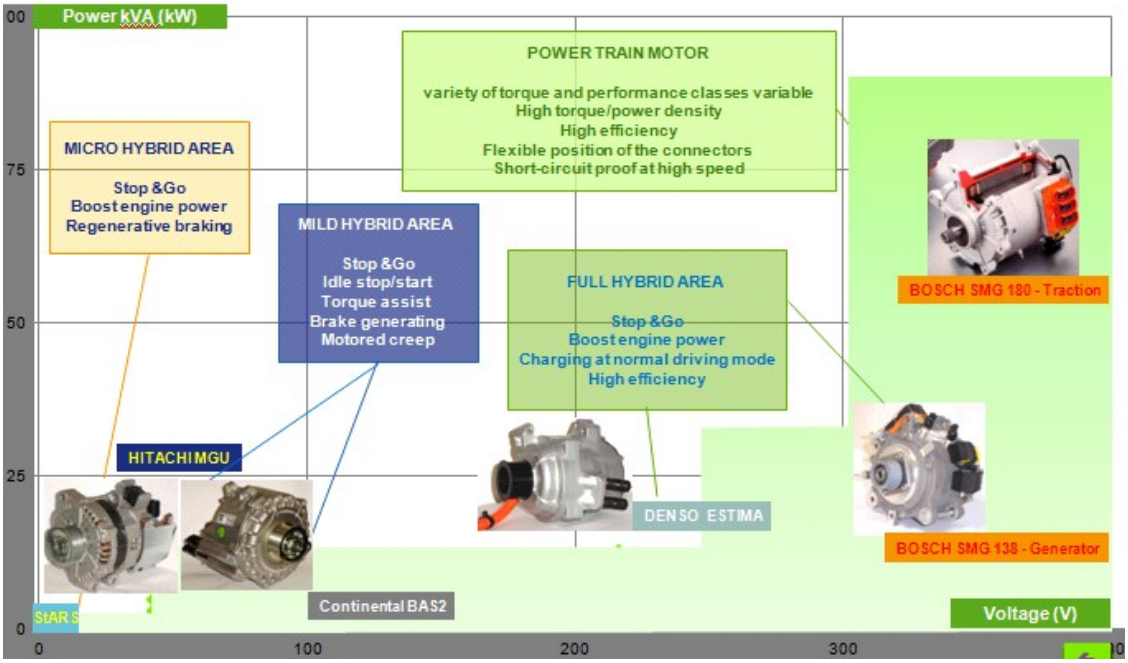

From micro hybrids to powertrain traction motors.

In the MAG-DRIVE BSG investigation we looked four belt-driven devices. The electrical machines were produced by Hitachi, Bosch and Mobis. These motors where purchased on the open market from the OEMs. The rated power ranged from a low 5 kW to 82 kW, 32 kg Bosch SMG 180. These machines were all about 20cm long.

	HITACHI MGU GM BAS 1	BOSCH SMG 138 PEUGEOT Hybrid4	BOSCH SMG 180 PEUGEOT Hybrid4	MOBIS BSG KIA- HYUNDAI Hybrid
Motor peak power (kW)	5	20	82	8.5
Motor peak torque (Nm)	65	65	55	43
Position sensor	Resolver	Digital	Resolver	Resolver
Voltage application (DC V)	42	300	380	270
Body diameter (mm)	Φ151	Φ162	Φ220	Φ158
Net length (mm)	184	190	212	161.5
Cooling system	Air	Water	Water	Water
Mass (kg)	8.2	14	32	12
Volume (dm^3)	3.29	3.91	8.06	3.17

BSGs tested as part of the MAG-DRIVE project

Next we investigated the rotors. Here we were interested primarily (with regards to the MAG-DRIVE project) in the number of magnets, the magnet dimensions, the total weight of the magnets and the performance estimate in terms of W/g of magnets. Full details can be found in figure.

	HITACHI : MGU GM BAS 1	BOSCH SMG 138 PSA Hybrid4 Generator	BOSCH SMG 180 PSA Hybrid4 Motor	MOBIS BSG KIA- HYUNDAI Hybrid
Pole – pairs	8	4	6	4
Outer diameter (mm)	114.6	83.85	120	71.98
Thickness (mm)	56	82	120	82
Nb magnet	16	64	144	6
Magnet dimension (mm)	10,95x8x32	12x5x20	12x5x20	27x3x80
Type flux	Mixte	Surface	Surface	Surface
Magnet weight (g)	336,4 (Ferrite)	576	1296	291
Peak power (kW)	5kW @DC42V	20kW @DC300V	82kW @DC380V	8.5 kW @DC270V
Perfo.estimate (W/g)	15 (ferrite+ exci. current)	35	63	29.15

Results of our tests on the rotors of the BSGs.

The figure below shows the rotor a Nissan Leaf water-cooled permanent-magnet motor 80kW at 400V. The details of this particular motor are: sheet thickness: 0.35 mm, magnets: 8 x 8 surfacing flux of 29 mm x 16 mm x 4 mm and 16 mm x 16 mm concentrating flux of 22 mm x 8 mm x 2.5 mm

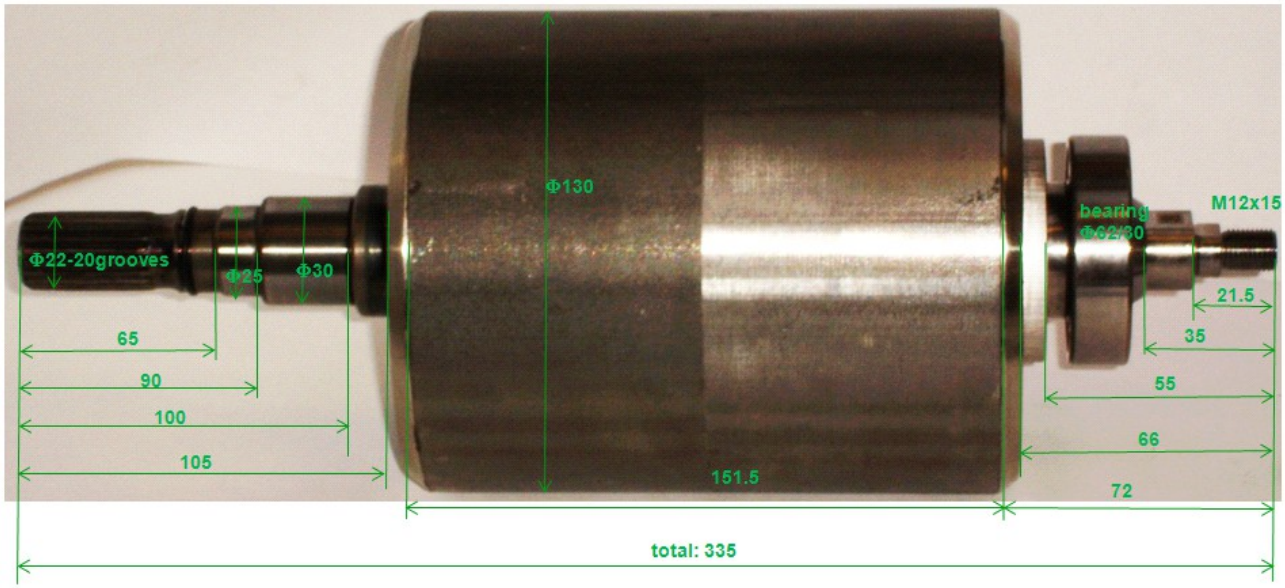

Rotor of Nissan Leaf electric motor

The best power density is achieved with the Peugeot Hybrid4 Nd-Fe-B rotor magnets with2.56 kW/kG, versus 0.61 kW/kG for the GM BAS1 with wound claw poles + inter claw poles ferrites rotor magnets.

2.2 Task 2.2: Design of thermal management for power electronics (M3 – M8)

Under the consideration were two types of the water-cooled inverters which can operate at the temperatures up to 80 ^{0}C: the 24 V B2-9 related to the crankshaft motor generator and the 270 V charger-inverter type CMG B2-6. Both Devices were developed by VALEO.

- Crankshaft Motor Generator B2-9:

  Voltage range 36/55 Vdc

  Typical voltage 48Vdc

  Maximum phase AC current 350Arms

  Temperature range -40°C / 80°C Water cooled

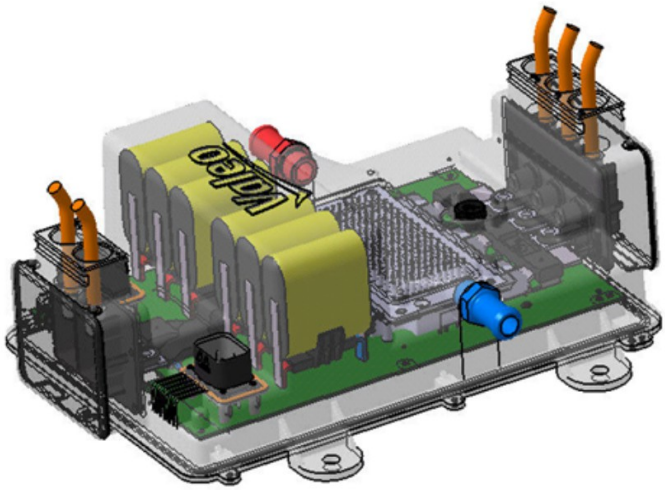

- 270V Charger inverter specification CMG B2-6

  Typical voltage 270Vdc

  Voltage range 220/300 V dc
  Maximum phase AC current 260Arms
  Temperature range -40°C / 80°C Water cooled

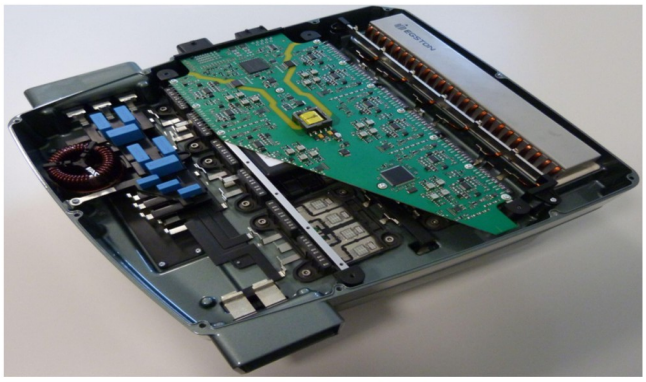

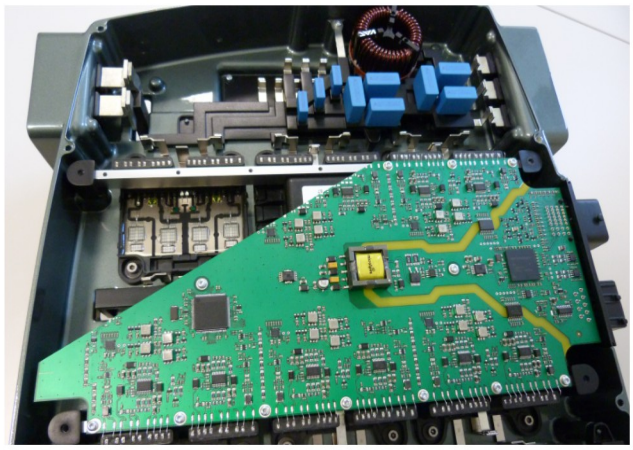

2.3 Task 2.3: Assessment of currently available permanent-magnet (M1 - M8)

RE-Fe-B-based magnets were taken from some of the motors and sent for a full chemical analysis. The results are shown in the tables below.

element	*element concentration [weight-%]*	*absolute measurement uncertainty [±weight-%]*	*limit of detection[1] [weight-%]*	*Limit of quantification[2] [weight-%]*
Al	0.21	0.01	0.004	0.01
B	0.91	0.03	0.01	0.02
Ce	< LOQ[2]	-	0.002	0.004
Co	2.19	0.02	0.001	0.003
Cu	0.19	0.01	0.003	0.008
Dy	10.42	0.34	0.0001	0.0006
Fe	59.64	0.72	0.005	0.006
Ga	< LOD[1]	-	0.02	0.04
Gd	0.02*	0.01	0.001	0.002
La	0.02*	0.01	0.001	0.003
Nd	19.04	0.58	0.005	0.015
P	< LOD[1]	-	0.004	0.01
Pr	0.07*	0.02	0.01	0.02
Sm	< LOQ[2]	-	0.002	0.004
Tb	< LOQ[2]	-	0.004	0.007
Y	0.07	0.01	0.0001	0.0002
Zn	0.14	0.01	0.001	0.001
Zr	0.03	0.01	0.001	0.002

Remarkably high Dy content in excess of 10 wt.%. This is approximately twice as high as we were expecting. The quantities of the other elements are in line with expectations.

WP 3: Route I – The Oxide Route (M1 - M30)

WP Leader: Wolfgang Kochanek (KE)

Summary of Results

The primary objective of the WP 3 was to produce nanocrystalline hard-magnetic material by applying the Kochanek process which is based on the reduction of oxides. The results of extensive experimental investigations revealed that samarium oxide could not be reduced in any form at any conditions, hence the conclusion was drawn that the samarium-cobalt magnets could not been made by means of the oxygen-reduction process. It was also demonstrated that the reduction of neodymium oxide was relatively low, therefore an additional infiltration of the neodymium nanoparticles is required in order to get the optimum results. It was decided to achieve this goal by performing the so-called wire-explosion experiments, where the required nanoparticles are formed upon the applying an extremely high electrical voltage between the two ends of a ribbon made of respective material. The resulting pulse current yields a decay of the ribbon into nanoparticles. The required ribbons were produced by spark-plasma sintering. Finally, we applied the Kochanek process to prepare the demonstrator magnets. The analysis, based on the scanning-electron microscopy and magnetic measurements, proved the route, developed in the frame of the WP3, promising for a massive production of permanent magnets, although further improvements in a reduction of the oxygen content, enhancement of the density, and of the amount of the hard NdFeB phase in the magnets are still required.

There were no deviations from the objectives and task given in Annex I.

Details for each Task

3.1 Task 3.1: Preparation of test cores from rare-earth oxides (M1 - M12)

The Kochanek process is based on the reduction of metal oxides. Therefore the feed stock for the Sm2Co17 consists of Sm2O3 and Co3O4 with organic compounds and of the Nd2O3, Fe3O4 and B with organic compounds in the case of the Nd2Fe14B. The main challenge consists in the reduction of the rare-earth oxides which have a high thermodynamic stability. The Gibbs free energy are 1085,3 kJ/mol and 1009,6 kJ/mol at room temperature for samarium and neodymium, respectively, indicating that the reduction under this conditions is thermodynamically not favourable With rising temperature the Gibbs free energies drop only a little. At 1800 K they still reach 844,5 kJ/mol for samarium and 858,6 kJ/mol for neodymium which does not significantly improve the thermodynamically conditions for reduction and suggests the equilibrium to be far on the left side of the reaction.

In the case of samarium a series of experiments was conducted which produced a total of over 40 samarium oxide based samples. The researched parameters in these reductions include temperature in a range from 650°C up to 1360°C, reduction duration from 3 h up to 6 h, precursor density from 3.29 g/cm3 up to 4,19 g/cm3 and different compositions of additives. Regardless of all the variations of parameters the weight loss measurements clearly proved that no samarium oxide reduction could be achieved as presented in the following XRD patterns:

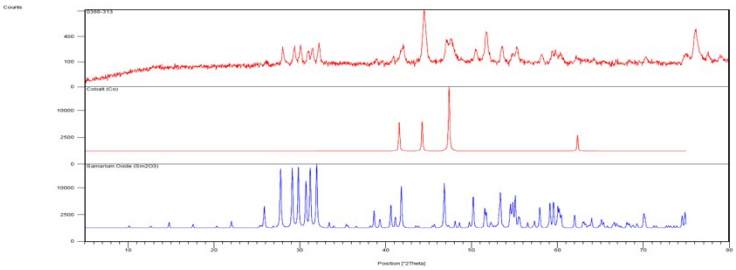

XRD of Sm2O3 Co3O4 reduced at 1200°C for 5h

Hence, we conclude that no samarium oxide can be reduced in order to apply the Kochanek process for making the Sm2Co17 magnets.

In the case of neodymium a series of experiments was conducted which produced a total of over 250 neodymium oxide based samples. The researched parameters in these reductions include temperature in a range from 650°C up to 1360°C, reduction duration from 3 h up to 9 h, precursor density from 1,47 g/cm3 up to 3,49 g/cm3, precursor particle size from roughly around 100 nm up to 5 µm, homogeneity of precursor material varied through the preparation process and different compositions of additives. Depending on these parameters a neodymium oxide turnover rate from 0% up to 20% could be achieved. The turnover rate was determined through the weight loss of the samples during reduction process. Simple by hand prepared samples achieved if at all only a low turnover rate. The highest neodymium oxide reduction rate could be reached through application of the more complex Kochanek process which yielded smaller particles and a higher homogeneity. At high temperature and long duration these samples reached a turnover rate close to 20%. The sample consisted of Nd2O3, Fe3O4, B and organic additives and was prepared according to the Kochanek process. The starting density was 3.11g/cm3 with a height of 6.06 mm and a diameter of 13.00 mm. After reductive treatment at 800 °C for 4 h a complete iron oxide turnover was achieved but none of the neodymium oxide. The density was lowered to 2.45 g/cm3with a height of 6.17 mm an a diameter of 12.63 mm. After pressing with 4.5 t/cm2 the sample showed a density of 4.47 g/cm3 with a height of 3.15mm and a diameter of 13.00 mm. A secondary reduction at 1360°C for 5 h yielded a neodymium oxide turnover rate of 8.6% determined through weight loss and a final density of 6.21 g/cm3 with a height of 2.86 mm and a diameter of 11.5 mm. Compared to the theoretical density of 7.65 g/cm3 the material reached 81.2%. The XRD analysis of the produced samples reflect the results obtained through weight loss measurements. Even though XRD does not allow to determine an exact neodymium oxide turnover rate the found phases depend on the composition and thus on the turnover rate. Samples treated with lower temperature whose weight loss measurements show no or little neodymium oxide turnover rate, show only iron and neodymium oxide phases in their corresponding XRDs. XRD results for materials prepared along the Kochanek process with high reduction temperature and a neodymium oxide turnover rate close to 20% show beside a main neodymium oxide and iron phase a small pure Nd phase:

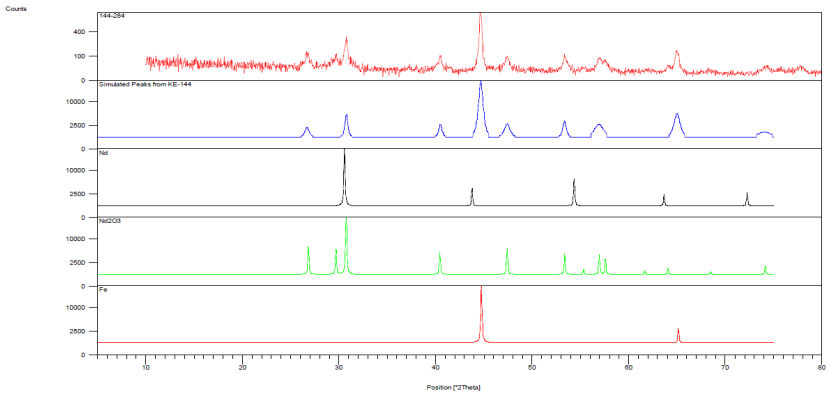

XRD of Nd2O3 Fe3O4 reduced at 1360°C for 9h

The EDS analysis showed a significant higher neodymium oxide turnover rate for oxides close to the surface. It was found that iron rich areas as well as iron lean areas achieved a similar neodymium vs. oxide ratio of about 7 : 3. This corresponds to a neodymium oxide reduction rate of 71% for oxides close to surface. The magnetic analysis of the samples show according to the previous results only a soft magnetic response due to the high iron content. The samples showed no coercivity and therefore no hard magnetic phases have formed.

We conclude that the reduction of neodymium oxide in the presents of Fe/Fe3O4 could be achieved up to 20% indicating that the thermodynamic stability is different in the presence of iron compared to pure neodymium oxide. To achieve a competitive hard magnetic NdFeB-material a neodymium oxide turnover rate close to 100% is needed since small impurities in the material have a negative influence on the magnetic properties. Trying to push the equilibrium of the reduction by high temperature is limited as we found out that the matrix starts to melt beyond1400°C. Which is supported by the iron neodymium phase diagram. Therefore we proposed an additional infiltration of the neodymium nanoparticles by performing the so-called wire-explosion experiments. The nano-sized powder was formed upon applying an extremely high electrical voltage between the two ends of a ribbon made of respective material. The resulting pulse current yielded a decay of the ribbon into nanoparticles. The required ribbons were produced by melt spinning.

3.2 Task 3.2: Preparation of hard magnetic materials (M9 – M18)

We used super-structured co-precipitated Nd2O3 /Fe3O4 material and conducted a series of experiments which produced a total of over 60 super-structured co-precipitated samples. The experiments where conducted in a temperature range from 700°C up to 1300°C and a duration of reduction of 4h. Samples chemical reduced with a temperature lower than 900°C re-oxidized on air at room temperature. The lower the reduction temperature the more rigorous the samples re-oxidized. This well known effect is based on the lesser sintering at lower temperatures resulting in a more reactive part. It is noticeable for the co-precipitated materials that the re-oxidation occurs at reduction temperatures up to 900°C. Comparable samples based on mere oxide mixtures did not re-oxidise at the researched temperatures with the lowest temperature being 600°C. This shows a more fine-grained particle size distribution for the co-precipitated materials. A SEM picture comparison between a neodymium oxide powder and the co-precipitated material illustrates the difference in particle size and therefore the reactivity due to a higher surface area. While the neodymium oxide particles size is above one micron the particle size of the co-precipitated material was within the sub-micron range:

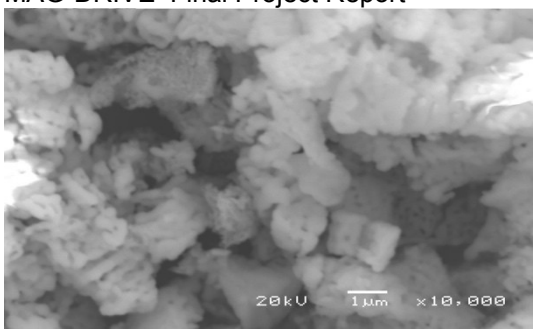

SEM image of neodymium oxide

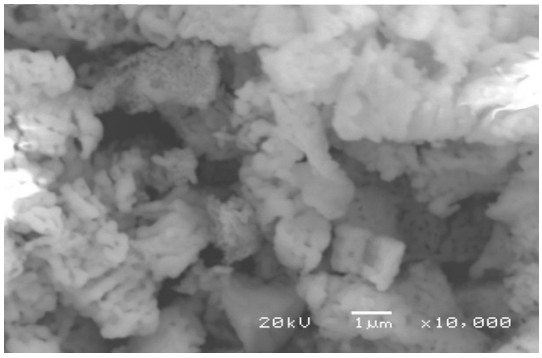

SEM of a super-structured co-precipitated material

Regardless of all the temperature variations and the higher reactivity based on smaller particles the weight loss measurement results of all super-structured co-precipitated precursors show a significant lower turnover rate instead of an expected increase in turnover. These losses in turnover rate can be explained through the XRD results. Instead of forming a Nd2Fe14B phase the reduction leads to a Fe main phase, a unexpected NdFeO3 phase, a Nd2O2S phase based on some sulphate impurities and a small pure Nd phase. Due to the formation of a NdFeO3 phase only an incomplete iron oxide reduction is achieved. This explains the significant lower turnover rate compared to samples based on oxide mixtures which in general achieve a close to 100% iron oxide reduction.

3.3 Task 3.3: Preparation of complex 3D-shaped permanent magnets for industrial use in Evs (M15 – M30)

During a wire explosion the “wire” reaches a temperature of more than 10^4 K with a heating rate of around 107 K/s. In general the explosion is achieved by the discharge of a capacitor through the conductive wire. Their capacity ranges from a fraction of a μF up to several hundred μF with storages voltages varying from a few kV to several hundred kV. Current peaks up to 50kA are common. The figure presents the voltage and current time dependence for a wire electrical explosion of a steel wire done with the experimental setup built for the MAG-DRIVE project. The capacitor was charged with 6kV and while discharging the current reached a maximum peak of almost 8kA. The whole process took less than 300μs:

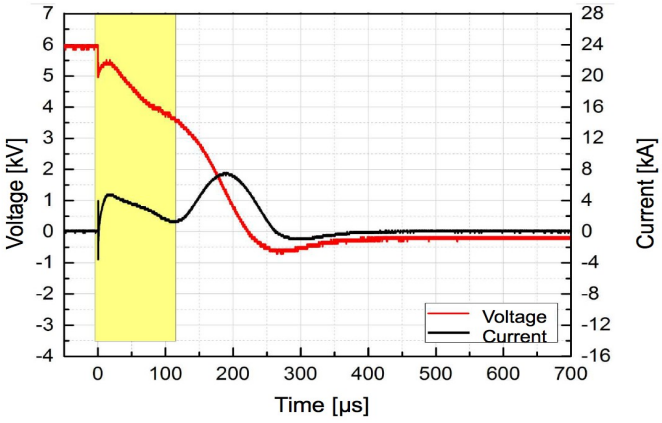

The voltage and current time dependence during a wire explosion.

The explosions took place in a special reactor, build for the purposes of the MAG-DRIVE project:

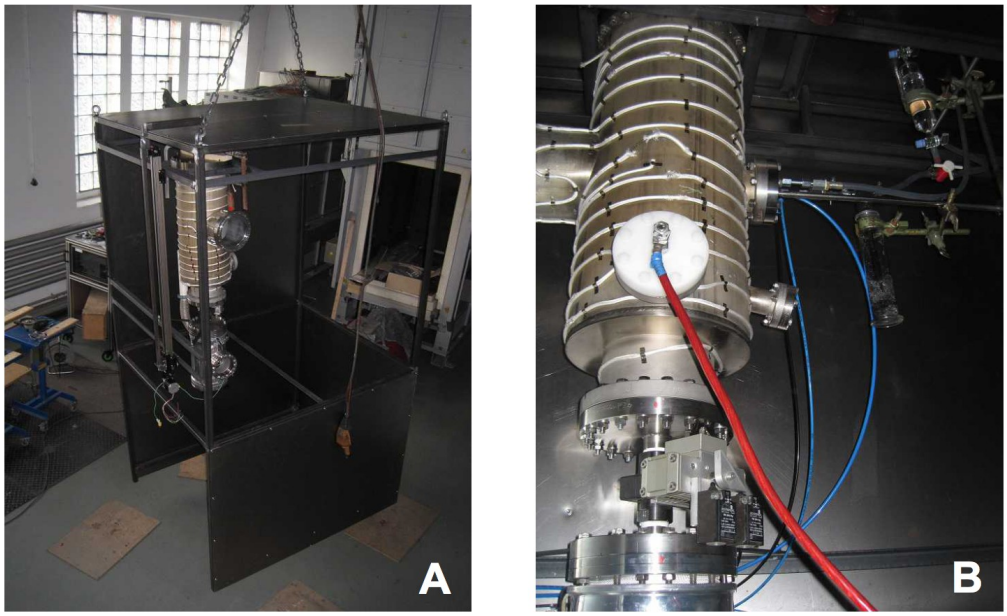

Wire-explosion reactor: the steel frame with the chamber and some shielding (A), the explosion chamber with the washing flask (B).

The explosion chamber was affixed inside a steel frame. Screwed on the whole outside of the steel frame were 3 mm thick steel plates to shield against electro magnetic waves. The explosion chamber was rendered inert with an constant Argon stream. Also hooked to the chamber was a pump that circulates the contained gas. In between the circulating gas stream was a washing flask to collect the product as shown in the following figure:

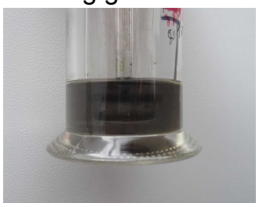

Extracted powder out of the explosion chamber.

The size of the resulting particles was determined by means of the scanning-electron microscopy yielding the assessment that the main fraction had a diameter between 20 and 150 nm with an occasional deviations up to 2 µm:

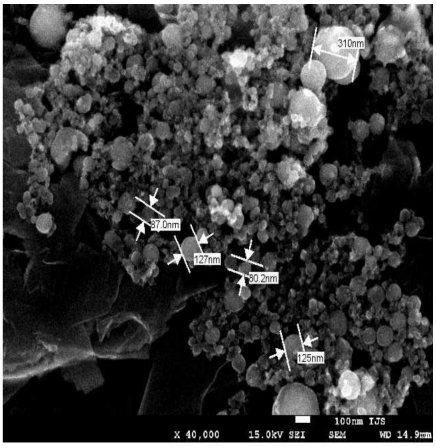

SEM image of nanoparticles produced via wire electrical explosion

The low density iron part for the infiltration with Nd based nanoparticles was produced according to the Kochanek process. The starting density of the disc shaped iron Kochanek parts was in the range of 2.72 to 2.98 g/cm^3, which equals a free pore volume of 61.4% to 58.8%. For infiltration a well stirred suspension of stabilized neodymium based nanoparticles was added drop-wise onto the Kochanek parts. To minimize the exposure to air the procedure was done in an argon ventilated glove box. The dropping speed of the suspension was adjusted to be as fast as the infiltration into the Kochanek sample itself. Dropping was carried out for as long as the suspension was sucked in.

The concentration of nanoparticles in the suspension needs to be 27,87% (v/v) for a free volume of 61.4% and 31.06% (v/v) for a free volume of 58.8% to be infiltrated in one session. Infiltration tests showed that suspension with such high concentrations of particles have a poor infiltration behavior. The parts will not get infiltrated thoroughly. Because of that a nanoparticle concentration of 15% (v/v) was used, which showed a good infiltration behavior up to the centre of the part in the preliminary tests.

The use of low concentration slurries made it necessary to infiltrate repeatedly. In between infiltration sessions the parts were dried until the cyclohexane evaporated. The procedure was repeated until the calculated amount of suspension was infiltrated into the Kochanek part.

After infiltration the samples were heat treated to take the organic components out of the part on the one hand and on the other hand to form the NdFeB hard magnetic phase. To evaporate the amines and to decompose the remaining organic components the samples were heat treated between 400 °C and 500 °C for several hours under hydrogen. Afterwards they were heated up to 850 °C for a duration of 10 hours under nitrogen to form the NdFeB hard magnetic phase. The parts reached a density from 3.85 g/cm^3 up to 4.26 g/cm^3 :

Final demonstrator after heat treatment

3.4 Task 3.4: Development of theory for hard magnets based on the Kochanek process (M18 - M30)

During the course of the project it was established that the reduction of oxygen might not be the most efficient procedure for the production of magnetic powders containing rare-earth and transition-metal elements. Therefore we successfully applied an equally innovative alternative by means of the wire-explosion experiment. However, we were still able to explain the reasons for a failure of the initially-proposed process in terms of a plausible theory.

The idea was to reduce neodymium oxide by exposing the samples to the elevated temperatures in the range from 650°C up to 1400°C in the H_2, N_2 and/or Ar atmosphere. At temperatures above 1000°C the reduction of neodymium oxide starts to begin. Unexpectedly at reduction temperatures of 1200°C and higher the turnover rates caves in not even reaching a complete iron oxide reduction anymore. This decrease in turnover rate was accompanied with a melting of the sample surface:

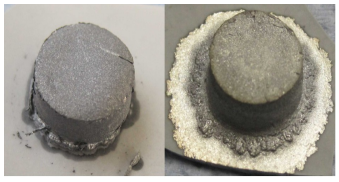

Reduction below 1200°C (left), reduction above 1200°C (right)

The molten surface could also be the reason for the low turnover rate, since it could be responsible for inhibiting the reduction by blocking the gas transfer between the centre of the sample and the surrounding atmosphere. An EDS analysis of the sample surface visualizes the molten surface as dark grey areas that mainly consist of iron:

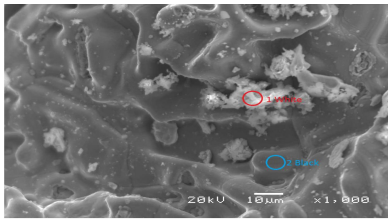

EDS of molten surface: 1. white area: 25.14 at% Fe, 22.02 at% O, 52.84 at% Nd 2. black area: 94.31 at% Fe, 1.63 at % O, 4.05 at% Nd

Even though the XRD and EDS results verified that a neodymium oxide reduction could be achieved to some degree there was no hint of a Nd2Fe14B hard magnetic phase in these results. Magnetic measurements of the samples confirmed these previous results as only a soft magnetic response, due to the high iron content, could be measured.

4 WP 4: Route II: The Nanoparticle route (M1 - M30)

WP Leader: Dana Vasiljević-Radović (ICMT)

Summary of Progress towards Objectives

The main objective of the WP4 was to obtain magnetic powder with the particle size of the order of magnitude of 1μm by means of innovative milling techniques. Towards this aim we analysed the commercially available equipment and decided for the most suitable technology which would serve as the starting point for further improvements. The application of this technology gave the satisfactory results in terms of the particle size close to the micrometer region. We quantitative analysed the size distribution and separated the powder.

There were no deviations from the objectives and task given in Annex I.

Details for each Task

4.1 Task 4.1: Analysis of the nano-milling technologies (M1 - M6)

The state of the art of different milling techniques that can be used to obtain sub-micrometer-sized nano-crystalline rare earth-transition metals magnetic materials was surveyed. Nanocrystalline NdFeB magnetic materials were considered since they possess the highest energy product of all the permanent magnets available today. We reviewed properties of different mechanical milling methods, including impact milling, ball milling, jet milling, roller milling, etc. We put the largest stress to the ball media milling and jet milling. The consideration includes the basic phenomena occurring in different milling procedures, the available equipment, including pros and cons for each type, different accompanying effects that may influence the quality of milling and the state of the art of experimental works in the field. Basic properties of NdFeB sub-micrometer and nano-powders were reviewed from the point of view of their influence on the production of permanent magnets. We performed also numerical simulation of different grinding and milling procedures by applying the the discrete element method. Based on the survey including the properties of both the powder material to be processed (brittleness, flammability, toxicity, etc) and the available techniques, we decided for the equipment most suitable for the use in our own experiments with NdFeB. It is a FRITSCH Planetary Micro Mill PULVERISETTE 7 fabricated by Fritch GmbH from Idar-Oberstein, Germany. The reasons for the decision are the following:

The grinding of materials down to the nano-meter range requires very high application of energy and therefore significantly higher rotational speeds than those allowed by typical planetary mills. Conventional planetary ball mills are characterized by grinding bowls that are clamped to the sun disk. This limits the maximum possible rotation speed because of a specific speed limit, the centrifugal forces acting on the bowls will be so great that the clamping of the bowls can no longer hold. Sinking of the grinding bowls into the sun disk of the mill solves these problems. In this construction, the centre of gravity of the bowls lies in the plane of the sun disk. The centrifugal force arising generate significantly lower overturning moment, which in turn allows the mill to run at significantly higher speed. As a result, this mill attains a speed of up to 1100 rpm, reaches centrifugal accelerations of up to 95 times the force of gravity, making the energy application approximately 150 % greater than conventional planetary mills. This significantly reduces the grinding time to reach the nano-meter range. For certain materials, as is NdFeB, brittle and hard, we think that only this level of energy application even allows the milling to NPs range. Grinding bowl size is 80 ml, ant it is made from tungsten carbide (WC). Grinding balls are from the same material. There are 2 bowls, max. sample quantity is 5ml and min. sample quantity is 0.5 ml. In bowls dry and wet grinding can be performed. We bought special emptying device which enables a quick and easy separation of the grinding balls and suspension. Grinding bowl is tightly sealed so that even grinding in suspension without any additional sealing is possible. Lead is equipped with pressure and temperature sensors and has a bleeder valve so that any overpressure in the bowl can be equalized in a controlled fashion. These features allow grinding in an inert atmosphere.

4.2 Task 4.2: “Light-gas” milling and comparison studies (M6 - M20)

The milling experiments were performed by the use of a JET-mill. The milling was accomplished by the use of light-gas milling of HD Nd-Fe-B material using a production-scale JET-mill. The comparative experiments were performed in the company Netzsch from Hanau in Germany, where they applied their ConJET dry grinding machine.

The starting material for the JET milling experiment was chosen to be a Magneti-standard NdFeB material with a low Dy content (1 wt. %). This material was chosen due to low intrinsic coercivity (Hcl)- owing to the low Dy content. 50 kg of NdFeB flakes was HD processed for the experiment,

The smallest ConJet produced by Netzsch, ConJet 10, was used for the experiments. In contrast to a fluidized-bed Jet mill, ConJet does not have a fluidized milling chamber with a fluidization nozzle on the bottom and a classifier on the top. The milling chamber is located around the classifier, with an increased number of nozzles. The milled powder particles path is therefore set longitudinal to the classifier, by which a sharper cut point of larger particles can be achieved compared to a fluidized-bed JET mill. In order to avoid oxidation of the incoming HD flakes and the collected (milled) powder, the whole mill was enclosed in a flexi glass bell, filled with inert atmosphere. The milling parameters were as follow:

- Milling gas N2, 99.95% purity (open circuit).
- Nozzle diameter: 1.2 mm.
- Nr. of nozzles: 5.
- Nozzle pressure 7 / 8 bar
- Classifier speed: 16,000 RPM/ 12,000 RPM / 3,000 RPM / 6,000 RPM / 9,000 RPM.
- Milling chamber pressure: 0.2–0.29 bar

The following two experiments were declared as a successful run:

- Ex1: Classifier: 16,000 RPM / p(nozzle): 8 bar / productivity: 0.2 kg/ h / D(observed) < 3 µm
- Ex2: Classifier: 6000 RPM / p(nozzle): 8 bar / productivity: 2 kg/ h / D(observed) < 8 µm

4.3 Task 4.3: Separation of magnetic particles (M12 – M24)

The first step in the magnetic-particles separation is the analysis of the powder size. We performed the on-site experiments with the SEI LOT Phenom PRO. The Ex1 (6,000 RPM / p(nozzle): 8 bar / productivity: 0.2 kg/ h) and the Ex2 (6000 RPM / p(nozzle): 8 bar / productivity: 2 kg/ h) materials were analysed. Although the Ex2 material obviously consisted of small particles, the productivity was too low, hence the average measured particle size was between 3 and 5 µm, which is very close to the submicron region, estimated as the optimum to achieve the desired magnetic properties.

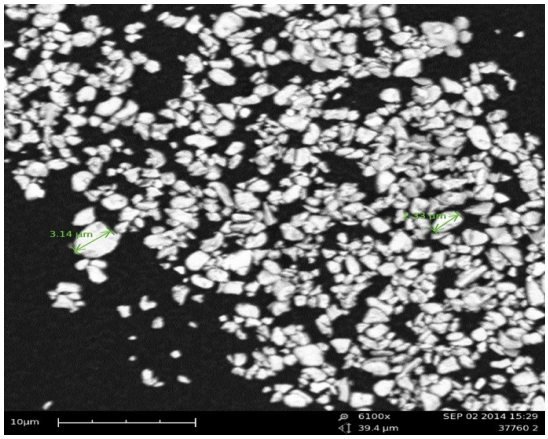

SEM image of the Ex1 milled powder

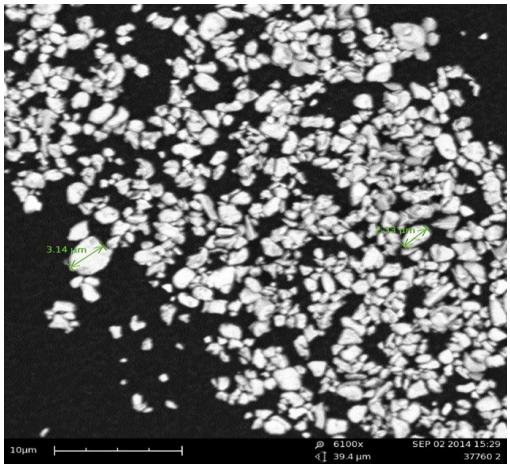

SEM image of the Ex2 milled powder

4.4 Task 4.4: Production of Dy-diffused Nd–Fe–B magnets (M20 – M30)

The essential step was to separate the particles of the desired size from larger suspension volumes using a process combining sedimentation and membrane filtration, which is schematically presented in the following figure:

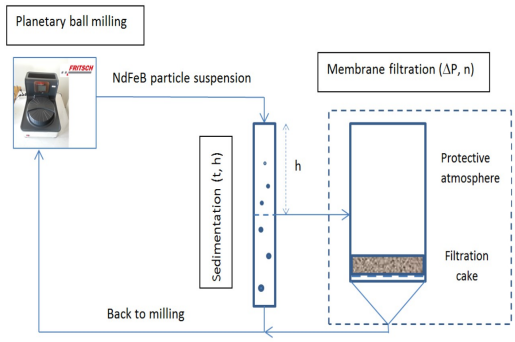

Scheme of the nanoparticle separation process for NdFeB magnetic material.

NdFeB particle suspension after surfactant-assisted wet milling is allowed to sediment for time t, then the upper portion of the suspension corresponding to height h is decanted and filtered in protective argon atmosphere under pressure ΔP through a membrane with a specific pore size. The process is repeated n times with the settled slurry and filtrate returning to another milling cycle. The filtration cake is composed of particles having a size distribution determined by sedimentation and filtration parameters. After filtration, polycarbonate membrane with the filtration cake consisting of NdFeB particles was immersed in 25 mL of chloroform to dissolve the membrane and disperse the particles. The resulting suspension was sonicated for 5 min and investigated with Zeta Sizer Nano ZS90 using a 1:10 dilution ratio. The resulting particles were characterized by the average diameter of 315 nm with most particles falling in the range from 200 to 500 nm:

		Diam. (nm)	% Intensity	Width (nm)
Z-Average (d.nm): 405.7	Peak 1:	315.5	100.0	74.02
PdI: 0.432	Peak 2:	0.000	0.0	0.000
Intercept: 0.912	Peak 3:	0.000	0.0	0.000

Result quality : Refer to quality report

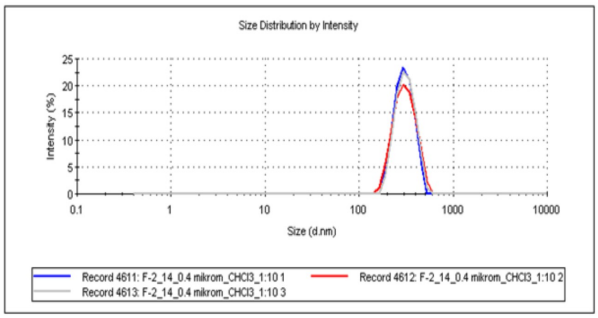

Nanoparticle size distribution determined by Zeta Sizer Nano ZS90 (Malvern Instruments) using chloroform as the carrier liquid.

Such magnetic powder exhibits the desired properties, the only obstacle for an eventual massive production are relatively small quantities of the produced material, which calls for further investigations towards scaling up the involved procedures.

5 WP 5: Route III: The HDDR+SPS route (M1 - M30)

WP Leader: Allan Walton (UOB)

Summary of Results

Hydrogenation Disproportionation Desorption and Recombination (HDDR) is a high temperature hydrogen treatment that utilizes the ability of materials such as Nd-Fe-B to readily absorb and desorb hydrogen at elevated temperatures which results in a fine grained material with very interesting magnetic properties.

It was found that the optimal processing conditions for the material with a reasonably low Dy content were the temperature of about 880 °C, with a disproportionation pressure of 1500 mbar, recombination under vacuum and quick cooling upon completion. However, by increasing the Dy as well as the the Co content the required applied pressure should be increased in order to complete disproportionation.

In order to fully exploit the potential of the material, it is highly desirable to align the particles prior to the final compaction. The result of the conventional spark-plasma sintering is an isotropic green compact, therefore we developed a method to pre-align the starting HDDR powder in the presence of an external magnetic field as described in detail within the Task 5.2.

There were no deviations from the objectives and task given in Annex I.

Details for each Task

5.1 Task 5.1: HDDR processing conditions (M3 - M15)

In this task the processing conditions for each step of the HDDR process were optimized for a range of different Nd-Fe-B magnet compositions including primary cast materials and secondary scrap sintered materials. The cast material includes a range of ternary alloys that can be altered with alloying additions to optimize the HDDR reaction. A range of sintered magnets have been used with low Dy levels.

The aim of this task was to avoid over-processing of the Nd-Fe-B material during each step of the process without foregoing the anisotropy that can be developed in HDDR powders. The disproportionation step was monitored using mass-flow controllers and a thermocouple for each chosen composition. The impact of the processing temperature and hydrogen pressure has been assessed in terms of their ultimate value, ramp rate and hold time during the disproportionation and recombination reactions. The impact of each of these variables on the microstructure has been determined with the aim of minimizing the size of the Fe, Fe2B and the Nd hydride rods in particular, prior to desorption. In a similar fashion the pressure-reduction rate and quench rate for the desorption step was monitored in order to minimise grain growth on formation of the Nd2Fe14B phase during the recombination reaction. The magnetic properties of the HDDR powders were measured in WP6 to assess the level of anisotropy that was developed for each composition and set of processing parameters.

Three compositions of Nd-Fe-B magnets were chosen for the trials. Two sources from large sintered blocks of Composition A - $Nd_{13.4}Dy_{0.8}Al_{0.7}Nb_{0.3}Fe_{78.5}B_{6.3}$ (at %) and Composition B – $Nd_{12.5}Dy_{1.8}Al_{0.9}Nb_{0.6}Co_{5.0}Fe_{72.8}B_{6.4}$ (at %). The first composition was very low in Dy as the target of this project is to lower the Dy content of fully dense sintered magnets. The second composition was chosen as the Dy content is slightly higher but still below the average Dy content measured across a range of mined sources (Wang 2013). Following on from this "real" scrap magnets were processed based upon voice coil motor magnets from hard disk drives. These were chosen as hard disk drives represent the largest source of sintered Nd-Fe-B from consumer products, they are collected in large quantities for data removal and there is relatively little variation in composition from product to product.

The HDDR processing conditions have been optimized for the processing of 20g sintered Nd-Fe-B batches of Composition A (low Dy). This was achieved by changing the process temperature (830-930 °C), disproportionation pressure (1000-2000 mbar), recombination pressure (0-350 mbar) and recombination time (0-30 mins) in order to produce the greatest magnetic properties. The optimal process conditions for Composition A were found to be at 880 °C, with a disproportionation pressure of 1500 mbar, recombination under vacuum and quick cooling upon completion. The voice coil motor magnets with a similar composition also processed successfully within the optimized parameters. Composition B which contains higher Dy and Co content, however, required a higher hydrogen pressure in order to complete disproportionation. By increasing the disproportionation pressure to 2000 mbar as required by Composition B, samples of Composition A exhibited lower remanence and were less anisotropic due to over-processing.

Having tracked the disproportionation reaction of the various sintered, book mould and strip cast starting alloys, it could be observed that the reaction kinetics were strongly affected by composition, rare earth content and initial microstructure. It was found that for the cast starting materials, the microstructure had the largest effect on the disproportionation reaction when compared to rare earth content. Strip cast alloys initiate disproportionation at lower hydrogen pressures than conventional book mould cast alloys which could be attributed to the much smaller grains in the strip cast material allowing for fast propagation of the disproportionation reaction through the matrix grains. Increasing neodymium content in ternary alloys increases the rate of reaction for hydrogen decrepitation but delays the onset of disproportionation. This can be attributed to the excess of Nd-rich grain boundary phase which reacts readily during hydrogen decrepitation but acts as a transport medium for hydrogen before disproportionation initiates within the matrix grains. For sintered magnets the additions of Co and Dy also delay the onset of the disproportionation, requiring an increased hydrogen pressure to initiate the reaction.

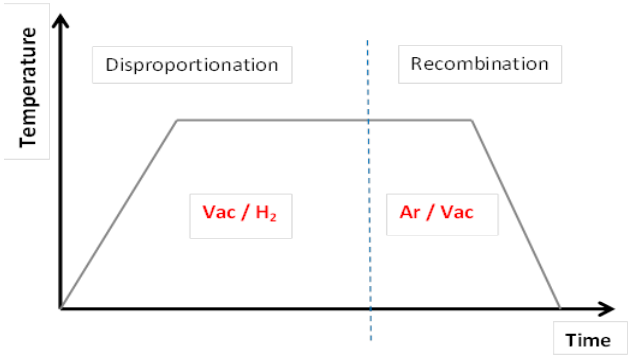

A typical HDDR schematic, showing the main variables as temperature, time and pressure

5.2 Task 5.2: Alignment and pressing of green compacts (M9 - M18)

For the production of aligned green compacts suitable for spark-plasma sintering (SPS) compaction, anisotropic HDDR powder was produced. The HDDR powder was a mixture of coarse and fine particles when removed from the processing furnace, and so it required breaking down using a pestle and mortar to remove any agglomeration. After 5-10 minutes of light grinding, the powder was suitable for green-compact production. 15 g of the HDDR powder was then loaded into a neoprene isostatic press bag and filled to tap density. A rubber bung was then pushed into the top of the press bag to a tight fit and then sealed using electrical tape. The seal was to ensure that liquid could not be introduced to the sample during the pressing stage and also prevents oxidation when the sample is prepared under an inert atmosphere. The sealed press bag was then placed inside the coil set from a capacitor-discharge pulse magnetiser. This piece of equipment consists of a large bank of capacitors that when pulsed from a fully charged state produce a 9 T field through the copper coils in the direction from ceiling to floor. The sample was situated centrally within the coil and held in place using a wooden-support system to ensure that the press bag is kept

completely vertical. If the press bag was to lean to the side or be allowed to move then the alignment of the powder within the press bag would not be perfect. The capacitors were charged and discharged three times to pulse the powder particles three times. This allowed for full alignment of the powder particles in the upwards direction. The press bag containing the aligned powder sample was then placed inside the water-filled chamber of the isostatic press. The top ram was then inserted into the chamber and the pressure increased to 10 tons and held for 1 minute. The pressure was then very slowly released to prevent cracking of the sample as the walls of the neoprene isostatic press bag released from the surface of the sample. Once removed from the isostatic press chamber, the green compacts were ejected from the press bag and inspected. The green compact does not have a parallel flat top and bottom faces. This is due to a combination of the particle size of the starting powder, the magnetic field exhibited by the compact and the lack of a binding agent as used in bonded magnets. The powder particles in these regions follow the magnetic field lines of the bulk of the magnet, this reduces the density of the upper and lower regions of the green compact. There are a number of ways in which this problem could be addressed. Mechanical removal of the 'fluffy' end parts using a blade is possible; however, the overall alignment of the sample could be reduced during the cutting process as the powder particles are disturbed. The large variation in particle size could be impacting on the stacking of the particles during compression. By reducing the particle size it could be possible to produce better compaction under isostatic pressing.

When reducing particle size it was important to consider an appropriate milling technique. Wet milling techniques such as low-energy roller ball milling requires cyclohexane carrier fluid and milling times from 1-20 hours to produce a fine particle size. The powder would then become very fine, leading to an increased potential for oxidation and yield loss during the drying process in a vacuum port. Jet milling would produce a very fine powder with particle sizes close to 1 μm and below. These particles would be very susceptible to oxidation and unfortunately due to the low sample size (20g) jet milling is out of the scope of this work.

The milling process chosen for this work was a laboratory sized hammer mill. This milling technique utilises three rotating blade arms that grind the powder against a ring of teeth that line the internal wall of the mill. A 0.2mm hole size mesh is placed in the bottom of the mill for the milled powder to pass through and into a collection tube. The built-in speed control unit allows for careful control of the milling process to avoid sparking of the Nd–Fe–B during the grinding of the particles between the rotating arms and the integrated grinding teeth.

The hammer mill was run for 10 minutes to allow all of the HDDR powder to pass through the 0.2 mm mesh. Due to the depth of the teeth in the hammer mill, the HDDR powder became caught during the milling process, reducing the yield collected in the tube; however, blowing compressed air through the loading hopper released the powder from the teeth to continue the milling process. The milled HDDR powder was then passed through the isostatic pressing route described above. The reduced particle size allowed for better stacking of the powder and hence a more uniform green compact was produced. There was a small amount of fine particles remaining in the bottom of the press bag after the green compact was removed, however they did not form along the magnetic field lines, as in the previous samples. However, due to the lack of a binding agent and the nature of the pressing route the powder around the edge walls of the surface became loose as the compact was handled; therefore, an alternative pressing technique was also considered.

Uniaxial pressing using a 20-mm die set allows for a higher pressure to be used, as well as controlled specimen dimensions due to the polished internal wall of the die set and the upper and lower punch pieces. As with the conventional SPS compaction route, this preparation method produces isotropic samples as there is no current alignment field. However, the pressing force used with this press and die set is 20 tons, rather than the 0.5 ton compaction used with the graphite die sets. It can be observed that the green compact is very uniform in size and shape; however, as previously stated the magnet is isotropic in nature.

A possible solution to this is that a copper wire could be wound around the die set and an electrical current be passed through the wire during the pressing action to create a magnetic alignment field within the die set. Unlike the isostatic alignment route, where the powder is pulsed aligned before pressing, this route would maintain a constant alignment field throughout the entire pressing process; however, the alignment field would be much weaker.

A potential improvement for the isostatic pressing route would be to powder blend the HDDR powder with milled neodymium hydride powder. The hydride powder would serve two roles in this process, firstly due to the powder being soft and friable, it would potentially acts as a binding agent to keep the green compact intact during and after removal from the isostatic pressing bag. Also it would aid with liquid-phase sintering during the SPS process, improving the densification behaviour of the compact.

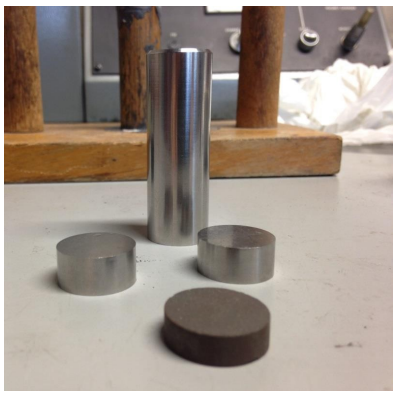

Nd–Fe–B green compact and die punch pieces

5.3 Task 5.3: Investigation of densification kinetics during SPS (M12 – M24)

The initial experiments were performed on large batches (400 g) of the low-Dy material with the composition $Nd_{13.4}Dy_{0.8}Al_{0.7}Nb_{0.3}Fe_{78.5}B_{6.3}$ since the main target of the project is to reduce the rare-earth content in the fully-dense sintered magnets. The magnetic properties, including anisotropy were reduced compared to the 20 g batches due to the highly endothermic nature of the recombination reaction. The temperature of the sample can drop by up to 100 °C during recombination, hence taking the sample out of the optimal processing window, leading to a loss in anisotropy.

The grain size was submicron however; hence it was a good material for initial SPS testing i.e. subsequent grain growth during SPS treatment could be checked.

The green compacts for the SPS treatment were formed by lightly grinding the HDDR-treated sample with a pestle and mortar. The powder was then loaded into a neoprene isostatic press bag and sealed with a rubber bung and electrical tape. The bag was then placed into a capacitor discharge pulse magnetiser and pulsed three times with a 9T alignment field. The sample was then pressed to 10 tons using an isostatic press. The green compact was then removed from the press bag and wrapped with a single layer of graphite paper and pressed into a graphite die. The die was then loaded into the SPS machine which was sealed and evacuated.

A range of SPS treatment conditions were trialled, and the best results were found after processing at 900 °C for 1 minute, the sample was cooled under vacuum and ejected from the graphite die. The density of this sample was calculated as 7.14 g cm-3, which was measured with a densitometer. The theoretical maximum density for Nd-Fe- B is ~7.5 g cm-3, so the sample was ~95% dense. The microstructure of this sample is shown in figure below. There is a mixture of very fine grains along with some large grains throughout the material. The average grain size was measured using the Feret diameter, and was calculated to be 0.75 µm with a standard deviation of 0.41 µm.

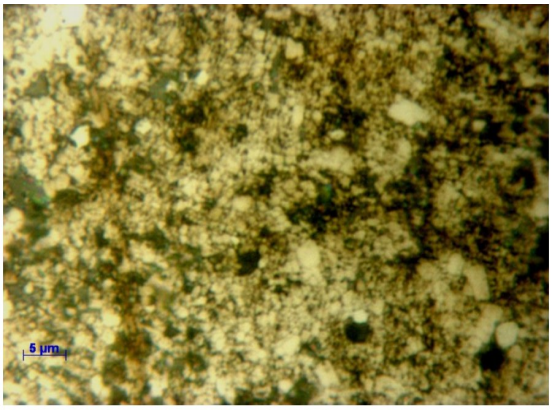

Micrograph showing the microstructure of the spark plasma sintered sample of HDDR-treatedcomposition A, using an optical microscope.

5.4 Task 5.4: Spark-plasma sintering of aligned green compacts (M18 - M30)

Like the conventional sintering, the spark-plasma sintering (SPS) is used to bind particles of material together into strong useable objects. This occurs through mass transfer at the atomic scale, acting to build ‘necks’ between particles. In addition to heating, pressure and electric fields are present during SPS to achieve the goal. The relatively high temperatures and sintering durations required to fully consolidate powders using conventional sintering techniques render the process unsuitable for the sintering of certain materials. For some materials, the sintering temperatures necessary to achieve full density are too high to sinter using conventional methods. In others, unwanted chemical reactions may occur during heating for long periods of time; and, where it is desirable for the properties or certain characteristics of the starting powder to be transferred to the final sintered compact, quicker processing times and/or lower processing temperatures are necessary to avoid any change in microstructure. For this reason, much of modern advanced materials sintering involves the use of Field Asisted Sintering Techniques (FAST). In contrast to the slow external heating methods employed in conventional sintering, FAST techniques employ the use of an applied electric current to produce high heating rates of up to 2000 K/min. Such heating rates are achieved through the application of pulsed current (from a few micro seconds to a few milli seconds) of extremely high current density -

up to several kA. This is possible due to the high electrical conductivity of the tooling involved and is therefore achieved without the need for high voltages (typically below 10 V). Powders and green compacts are usually sintered within a conductive die. In the case of an electrically conductive green body, energy is dissipated directly within the sample and the conductive die; whilst for electrically insulating green parts, the heat is generated through the Joule heating of the die and is transmitted by conduction to the powder:

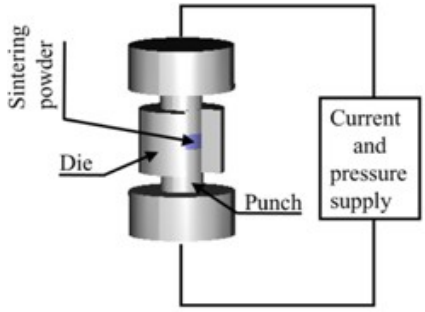

Schematic diagram of a pressure-assisted FAST process

The process yields a densification (shrinkage) of the exposed material. We applied the heating rate of 100 °C min^{-1} up to 900 °C and pressure of 50 MPa for four different powders:

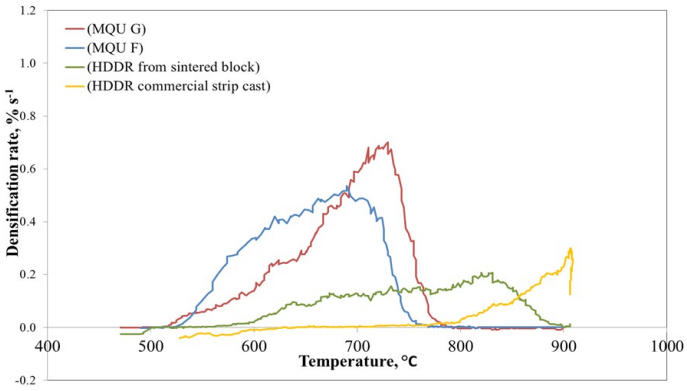

Densification rate curves plotted as a function of temperature for the four NdFeB materials

The fall of the rate of densification to 0 beyond 730 °C suggests that densification has completed. After sintering, the sample density was measured using Archimedes principle and confirmed to be near theoretical, hence applicable for the production of magnets.

6 WP 6: Microstructural and magnetic characterisation (M3 - M35)

WP Leader: Matej Komelj (JSI)

Summary of Results

This work package provided the service for WP3, WP4 and WP5 with constantly ongoing activities by means of analysing the structural and magnetic properties of the processed materials. In term of structural characterization the basic tool was the scanning electron microscope which makes us possible to qualitatively observe the microstructure, i.e., the phase composition, resulting from different processing conditions. By applying this technique we demonstrated the strength of the HDDR method in reducing the amount of the undesired soft-magnetic alpha-Fe phase. Advanced microscopy methods made us possible to quantitatively characterize the chemical compositions of the considered materials. Other techniques, like high-resolution transmission electron-microscopy (HRTEM) or laser confocal microscopy were used for imaging on atomistic level or of complex 3D shapes, which was important for the spark-plasma sintered compacts as presented in the description of the Task 6.2. Of equal importance as the microscopy were magnetic measurements. We relied on two different principles: the open-looped vibrating-sample magnetometer and the closed-loop permeameter. The former was more suitable for the samples in a powder form, whereas the latter was applicable for solid magnets. Both techniques were widely used throughout during the execution of the project. The particle size and surface morphology were of a great importance for the WP4. Different milling conditions lead to different particle sizes. It was very important to protect the magnets for electrical-vehicle applications against corrosion. An appropriate protection can drastically reduce a decay of a magnet due to environmental conditions as demonstrated in the Task 6.5.

There were no deviations from the objectives and task given in Annex I.

Details for each Task

6.1 Task 6.1: Scanning electron microscopy (M3 – M35)

Scanning electron microscopy is the single-most important analysing technique for materials science . The length scales involved at every stage of the procedure, from hundreds of microns to hundreds of nanometres, are well covered by this technique. The key information that was supplied here by the SEM technique relates to grain size and phase distribution. Of particular importance were the observations relating to book-mould-cast and strip-cast material. The SEM revealed the striking differences in microstructures that can be obtained with these techniques. Book-mould casting tended to produce larger grains, a coarser microstructure and more separated phases – and most importantly the presence of free iron, which is potentially at least very problematic for permanent-magnet production of any kind. The SEM studies revealed how strip casting, to a large extent, overcomes these problems.

By way of benchmarking the SEM technique was also applied to sintered magnets, where it was able to show that sintered Nd-Fe-B magnets also consist of two main distinguishable phases: Nd2Fe14B matrix grains surrounded by a network of Nd-rich triple junctions and grain boundaries.

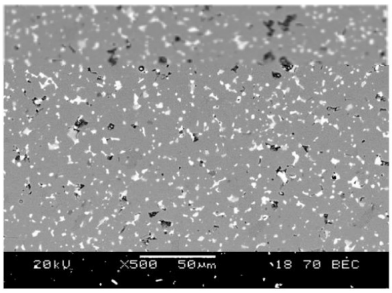

Backscattered SEM micrograph at x500 magnification of sintered Nd- Fe-B consisting of two main phases with evidence of porosity.

When SEM is used to look at HDDR material, which is material on a sub-micrometre scale it shows very nicely that the HDDR process is successful in 'removing' the α-Fe from the starting microstructure. When the HDDR process is applied to strip cast material the SEM is able to show that the long, columnar grains are also absent from the microstructure and that this HDDR processed strip cast Nd-Fe-B could lead to better compaction using spark plasma sintering (SPS) as the regions of cavitation are not as significant as in HDDR processed book mould cast Nd-Fe-B.

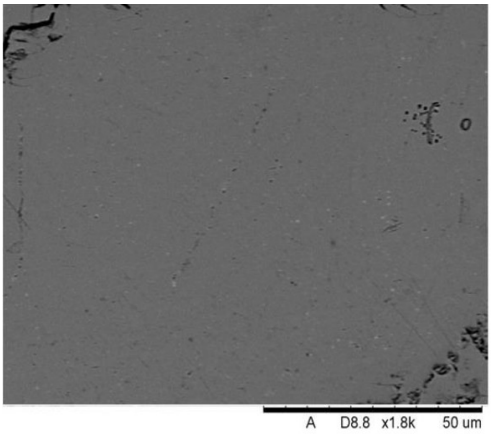

Backscattered SEM micrograph at x1800 magnification of HDDR processed strip cast

The SEM was also used to look at SPS samples of HDDR powder. This starting powder was found to have an ideal submicron grain size distribution, typical of HDDR-processed material. However, there was also evidence of explosive grain growth in some of these samples, particularly those processed at high temperatures. Again, SEM is an ideal technique for assessing materials in this way and provides a clear explanation for the lower-than-expected coercivity values, but with the advantage of providing us with a clear path to overcome the problem. In the case of the best samples achieved so far for HDDR powder and SPS, based on grain size alone, the retention of a proportion of fine grains which are of single-domain size in the best samples suggests that the magnetic properties of these samples can be improved.

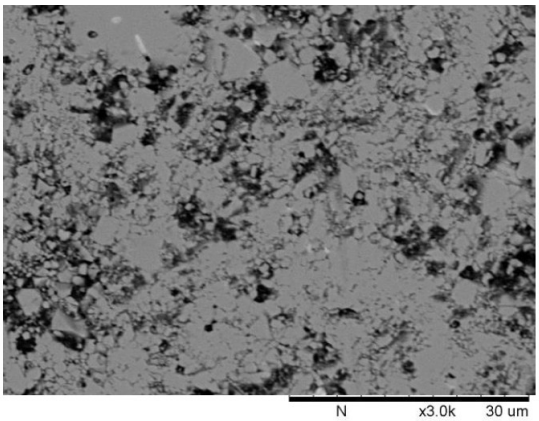

Backscattered SEM micrographs of HDDR-processed Nd-Fe-B consolidated using SPS at 900 °C for 10 minutes at magnifications of x3000

6.2 Task 6.2: Advanced electron microscopy (M3 - M35)

Advanced electron microscopy includes techniques like energy-dispersive X-ray spectroscopy (EDXS), electron-energy loss spectroscopy (EELS), high-resolution transmission electron microscopy (HRTEM), Lorenz microscopy, Laser assisted 3D atom probe (3DAP) microscopy, and Laser confocal microscopy. EDXS and EELS are methods which make us possible to quantitatively analyse the scanning-electron-microscopy or HRTEM images in terms of chemical composition. HRTEM is suitable for detailed grain boundary and multiphase analysis and is excellent for location of defects, foreign bodies and interfaces between two phases. In addiction with the focused ion beam (FIB) it is an excellent tool for a sample preparation on the atomic level. Lorentz microscopy can be used to image magnetic domains in a structure, whereas the 3DAP microscopy enables exact elemental positioning within a solid sample.

Laser confocal microscopy can be used to obtain both high resolution optical images (2D) and 3-dimensional profiles by capturing and layering multiple images through a range of depths within the sample via optical sectioning. This technique allows the user to acquire image data and images from complex 3D shapes including surface topology and profiling as well as internal structure imaging. Initial work on SPS compacts revealed small regions of cavitation throughout the sintered sample, leading to a density lower than the theoretical maximum (7.19 gcm^{-3} compared to 7.50 gcm^{-3}). Using standard 2D laser imaging it was possible to locate one of these regions. The cavity was approximately 10 µm wide and 15 µm long. 3D laser microscopy on this area was performed, and is shown in the figure below. It can be observed that the centre of the cavity is very rough, consisting of a large pit of varying depth. It was also observed that there are multiple small holes/pits in the microstructure around the main cavity, which could be attributed to the redistribution of Nd-rich during the HDDR process from a large triple junction into a fine microstructure.

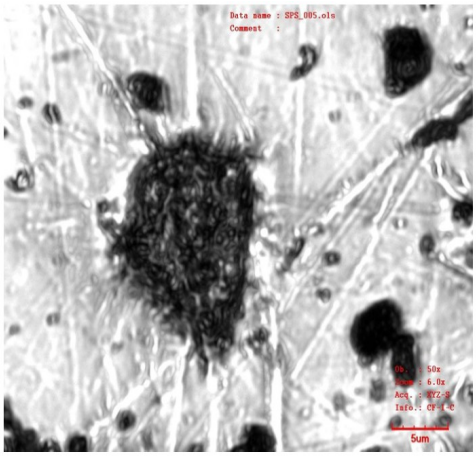

3D laser image of cavitation in an SPS compact

6.3 Task 6.3: Magnetic measurement (M3 - M35)

Magnetic measurements represented one of the most critical aspects of the project. We performed the so-called open loop measurements with the vibrating-sample magnetometer (VSM), and the closed loop measurement with the permeameter. One of the important tasks was to ensure that comparisons could be made between the two types of measurements; this is mainly because not every type of sample can be measured in both open- and closed- loop measurements. Powders, for example, could not be measured easily in a closed-loop permeameter measurement, whereas large samples, with dimensions greater than 5 mm (typically), could not be measured with an open-loop VSM.

A comparison between the results obtained by applying the two techniques was performed for various materials either utilized in sintered magnets (permeameter) or in a powder form (VSM) obtained after exposing the starting magnets to the HDDR process. Here we present the respective graphs for the composition A: $Nd_{13.4}Dy_{0.7}Fe_{78.6}Al_{0.7}Nb_{0.4}B_{6.2}$.

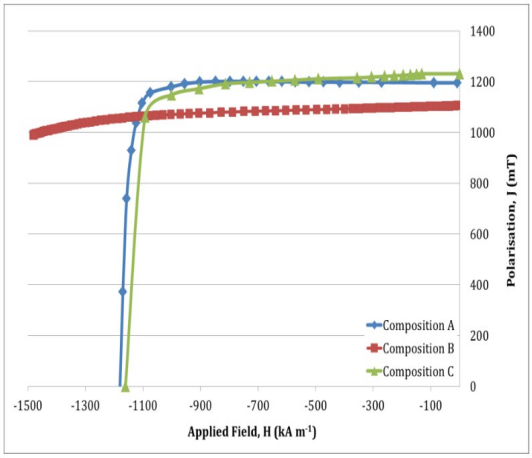

Demagnetisation curves for starting sintered materials of Compositions A, B and C as measured by applying the permeameter

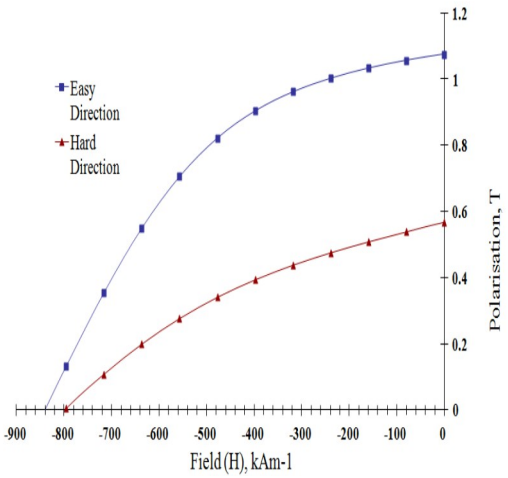

Demagnetisation quadrant for HDDR powder of composition A

The SEM imaging was proven as very efficient for the assessment of the particle size as shown in the following figure for the powder obtained by applying the wire explosion experiment:

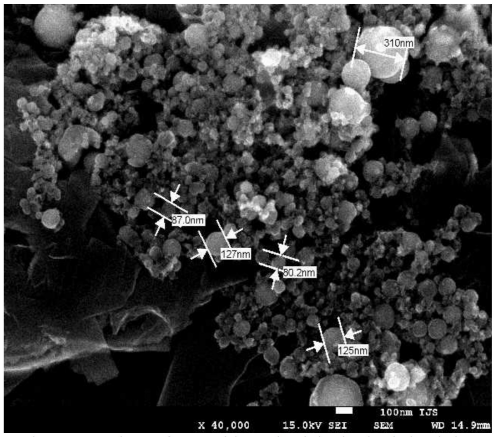

SEM image of nanoparticles produced via wire electrical explosion

Although this technique does not make us possible to determine an exact particle-size distribution, it is evident that the main fraction of the particles had a diameter between 20 and 150 nm with occasional bigger particles of up to 2 μm, which surface can be analyzed in detail:

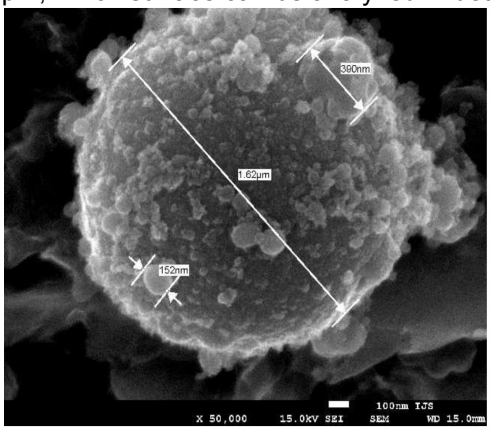

SEM image with a single bigger particle

However, a more detailed analysis required the application of the laser diffraction, which should, in principle yield the respective distribution. But the method turned out not to be as useful as expected because of the agglomeration, partly ascribed to the magnetic attraction:

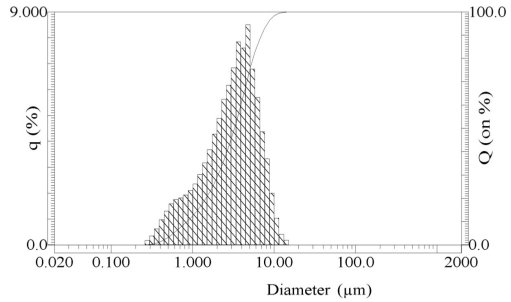

Laser diffraction analysis of agglomerates

6.5 Task 6.5: Corrosion tests (M12 – M35)

Nd–Fe–B magnets require a protective coating / surface finish to minimize the effects of corrosion. Iron within the structure can 'rust', which causes a permanent structural change in Nd–Fe–B, which results in a permanent weakening of the magnetic performance – the worst case scenario is a total loss of magnetism. In order to determine the effect of corrosion on Nd–Fe–B magnets, numerous corrosion tests need to be employed. This is especially important for magnets that are supposed to be used in any type of electric vehicles.

For testing the corrosion resistance of magnets we had available multiple methods and tests. These were:

- Autoclave: 120 °C / 2 bar / RH 100%
- "HAST": 130 °C / 2,7 bar / RH 95%
- Environmental test: 85 °C / RH:85 %
- Salt spray test (Coated magnets)

We had to apply the following test procedures:

- Cleaning the samples
- Weighing 1 + dimensions (surface area)
- Test chamber (several days)
- Weighing 2 => weight loss / area

The corrosion resistance can be improved by using various coatings or by reducing the oxidation rate of the Nd-rich phase in the case of the Nd-Fe-B magnets. The latter can be achieved by substituting the respective phase by some other phase, or by minimizing the electrochemical potential between this phase and the hard-magnetic phase $Nd_2Fe_{14}B$, which is the driving force for corrosion. The figure presents the weight loss for some magnets with and without coating:

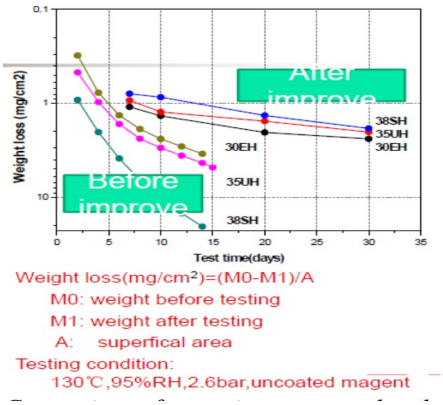

Comparison of corrosion on normal and improved magnets

7 WP 7: Production of Permanent magnets and Thermal Management Components (M12 - M30)

WP Leader: Irena Škulj (MAGNETI), Jean-Marc Dubus (VALEO)

Summary of Results

Once we succeeded to prepare magnetic powders with required properties via the three routes covered in the work-packages WP3, WP4 and WP5, of which the HDDR+SPS route (WP5) turned out to be the most effective, we focused on the production of magnets. The work was mainly done in the magnet-producing company Magneti with the required equipment, experiences and knowledge. After considering various possibilities it was decided to apply the press-less sintering with the additional post-sintering heat treatment, which was proven as beneficial in order to further improve the properties. However, it was found that the results considerably depended on the processing parameters, hence they should be tuned for a particular processing set-up.

The thermal management was realized in Valeo, where it was decided to apply the conventional solution, based on an inverter, composed of the power module and the control card, making up possible to manipulate the machine-stator phases for the production of either the mechanical or electrical power.

There were no deviations from the objectives and task given in Annex I.

Details for each Task

7.1 Task 7.1: Preparation of magnet-processing (M12 - M20)

On the basis of the performed experiments we decided to include in the production process for production of new magnets powder preparation (hydrogen decrepitation and milling) and heat treatments (sintering and heat treatment). Part of production for fine powders required HD plant and jet mill and magnet preparation part required moulds for powder packing and aligning and vacuum furnaces for sintering and heat treatments.

Requirements for equipment:

- HD plant: For the furnace to be able to carry on Hydrogen decrepitation would be important to be able to reach temperatures up to 1000°C and pressures up to approximately 3 bar. HD plant should be able carry out HDDR process to be able to improve magnetic properties.
- Jet mill: We tried to find the appropriate equipment for milling below 1 µm or less with Netzsch Company. The most promising proved to be CON JET. It was hard to define the needed specifications for the mill and milling medium.
- Moulds: It was proved that moulds with cavities for NdFeB powders made of graphite were satisfactory. In the case of press-less process there is no need for a big press with a magnetic field. All that is needed is a graphite mould with cavities and magnetiser to align powders when already in the mould. With this kind of technology the production is limited to relatively simple shapes of magnets.
- Furnace: Here we are talking about usual sintering furnace that is capable of reaching good vacuum and has options of fast cooling with Argon gas.

7.2 Task 7.2: Pressing, sintering and magnetization of samples (M14 – M24)

We decided for the press-less sintering technique. It was important to mill fine powders of the right chemical composition, and to sinter aligned powders into magnets. Throughout the process it was most important to follow the

milling step by particle-size distribution analyser. Throughout the process we performed the tests of the following properties: chemical compositions, density, shrinkage, magnetic properties, microstructural changes.

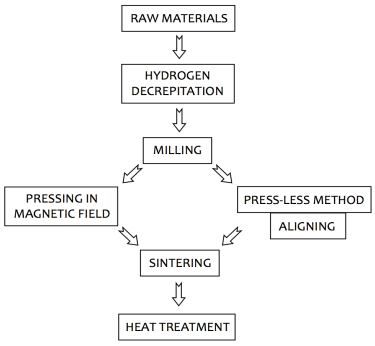

A schematic flow chart of the process for production of NdFeB magnets

7.3 Task 7.3: Assessment of permanent magnets (M20 – M26)

In order to determine the optimal processing conditions as well as processing techniques at particular steps of the procedure we compared different magnets:

Sintered magnets from ball-mill powders (iso-statically pressed on the left, press-less in the middle and on the right).

We found that the magnets sintered from ball milled powders and prepared through press-less method did not sinter at all; full density was not achieved. Therefore the magnets were not magnetic. For a comparison the powders were also pressed iso-statically and sintered. Magnets prepared via press-less method were too oxidized but magnet prepared via isostatic pressing had no hard magnetic phase Nd2Fe14B present in the microstructure. Powders prepared with ConJet in Netzsch were damaged during further processing and therefore not made magnets.

The final test was, of course, the magnetic measurement to prove the choice of the processing route and techniques. Here we present a comparison in the demagnetization curves of a magnet in as sintered state and after continued heat treatment:

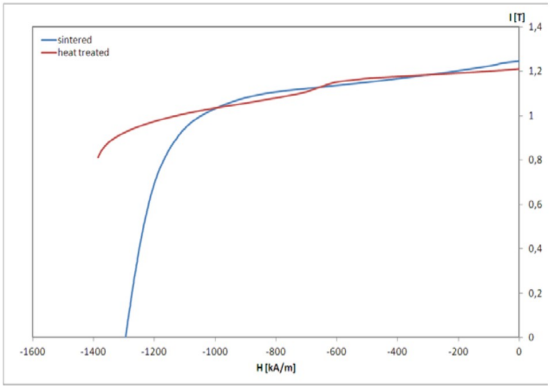

Demagnetization curves of a produced magnet before and after heat treatment

The measured properties were as expected:

- Br = 1,21 T
- bHc = 850 kA/m
- iHc > 1600 kA/m
- BHmax = 270 kJ/m3.

7.4 Task 7.4: Thermal management of power electronics (M18 – M28)

It turned out that the power electronics for controlling the electric-motor which consisted of the permanent magnets produced during the course of the MAG-DRIVE project was not as critical as it might be expected, therefore we sticked to the standard, water-cooled solution in terms of a commercially-available inverter. The inverter is composed of a power module which controls the machine-stator phases to produce mechanical or electrical power. The power module use depends on the voltage, either with the power Mosfet or IGBT that are driven by the control card.

The control card contains all the machine piloting algorithms in a microcontroller, as well as the rotor position sensor algorithms and the vehicle strategy, the battery state of charge, the machine temperature calculation, etc.

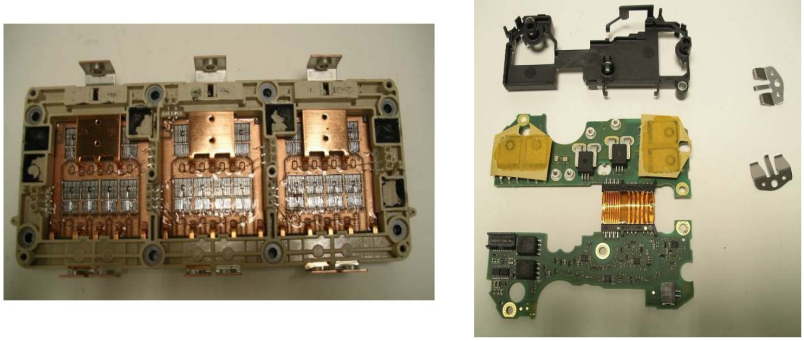

Power modules (left), control card (right)

7.5 Task 7.5: Optimisation of EM power density using new permanent magnets (M24 - M30)

We selected the optimal sets of the magnets produced during the course of the project. As expected the best results were achieved by applying the HDDR+SPS route from the WP5. The figure below presents typical locations of permanent magnets in the cross-section of an electric-motor rotor:

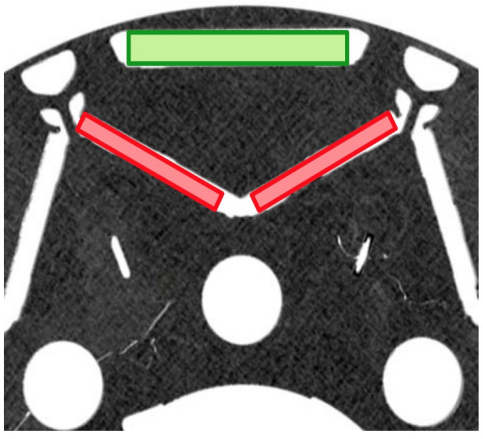

Cross-section of an electric-motor rotor presenting the position of permanent magnets.

Such configurations made us possible to achieve the power densities of up to 2.56 kW/kG.

Thermal behavior situation with 145℃ Heat-sink Ful l load

	ASIC DRIVER	MOS B+	MOS phase
Dissipated Power (W)	0.5	0.8	0.8
Max temperatures (℃)	158	147	150

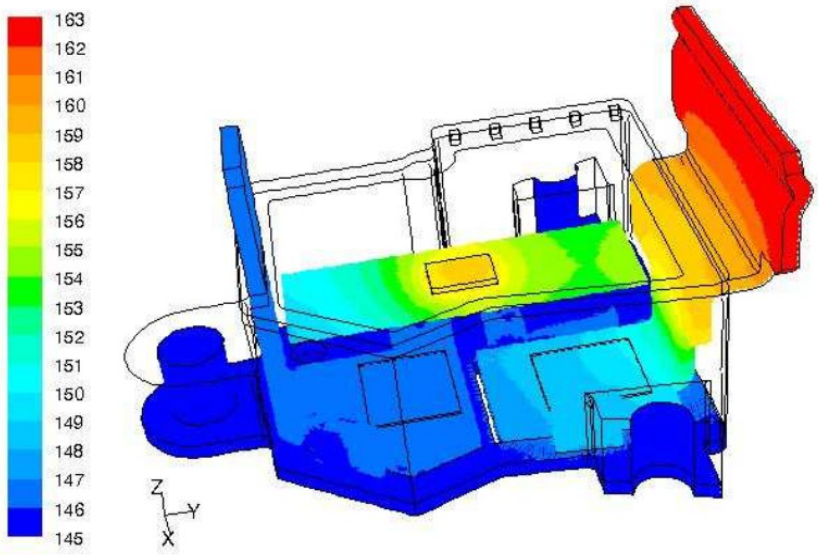

Study about the thickness of the lead-frames:

8 WP 8: Testing of the Magnets and Electric Motors in the Real-World Conditions (M24 - M35)

WP Leader: Jean-Marc Dubus (VALEO)

Summary of Results

This work-package was supposed to include the final research activities of the MagDrive project, since it was about testing and applying the magnets in electric motors, constructed in Valeo. It turned out to be completely successful since the delivered magnets passed all standard-prescribed tests, whereas the respective motor, performed according to specifications.

There were no deviations from the objectives and task given in Annex I.

Details for each Task

8.1 Task 8.1: Preparation for the tests (M24 – M26)

There were no special preparations needed for the tests of the magnets since all the required equipment was readily available at Valeo and Magneti. The magnetic properties were determined by applying the same techniques as described in the WP6, mainly by using the permeameter, designed for the so-called closed-loop measurements. A more dedicated was the device for the measurements bending force and displacement:

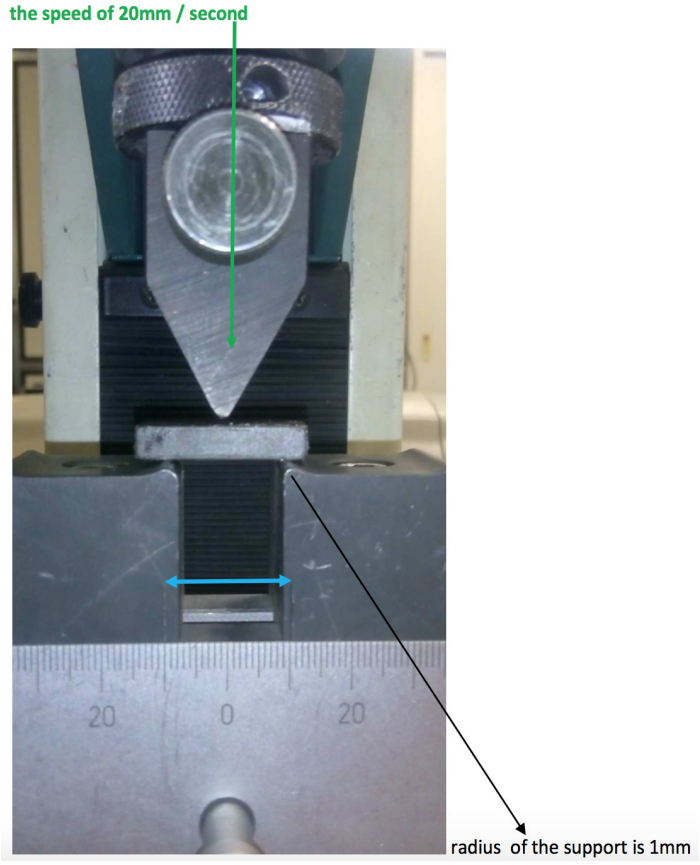

The device the for the measurement of the bending force and displacment

torque:

Data acquisition during the torque measurement

output efficiency:

The device for the output-efficiency measurements

and thermal properties:

The device for the thermal properties measurements

8.2 Task 8.2: Physical and magnetic properties of the permanent magnets (M26 – M28)

On the basis of the magnetic measurements on the powders, produced along the three routes, which were covered by the work-packages WP3, WP4 and WP5, we decided that the best magnets should result from the HDDR+SPS material. Hence we prepared bigger size magnets and cut them into smaller pieces that were appropriate for measurements and had their magnetic properties measured with permagraph at Magneti Ljubljana d.d.. Final magnets were additionally cut and ground to obtain a shape defined by Valeo, so that the diameters were about 40 mm. We ended up with 16 different magnets; four form each of the four different compacts related to the variation of the processing parameters. The following figures represent the measured demagnetization curves:

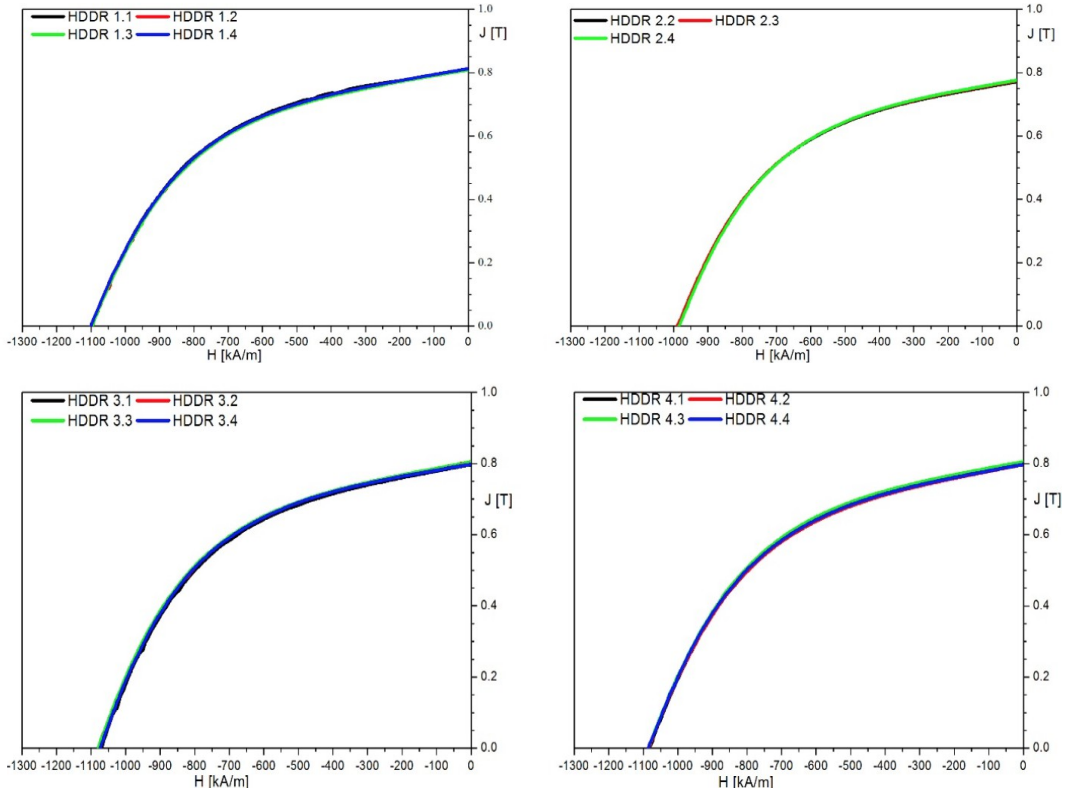

The demagnetization curves for different magnets produced from four different HDDR+SPS compacts

The results revealed a pronounced homogeneity of the compacts reflected in a reproducibility of the results. Whereas the magnets from all four compacts exhibited nearly the same remanence values of 0.8 T, the compact 1 was distinguished by the highest coercivity of 1100 kA/m, following by the compacts 3 and 4 with slightly lower values. The magnets from the compact 2 had about 10% lower coercivity, thus they were least applicable.

8.3 Task 8.3: Corrosion properties of the permanent magnets (M26 – M28)

The standard procedure in Valeo to check the corrosion resistance of electric components is the salt-spray test. It makes us possible to check the ring/brushes-compartment tightness and the vulnerability of the machine face to the electro-corrosion.

Test conditions:

- Machine in rotation mounted in a specific angular position in a specific bench, with representative customer regulator plugs & an electrical circuit with a battery of 70 Ah, wiring of 35 mm2 2 m + 2 m,
- Cycle: 75 min (60 min running on alternator mode (ON), 15 min stopped (OFF))

- Phase « On »: Ambient temperature (*T*a) Salt mass concentration Pulverization pressure Salted water quantity Rotation frequency (*n*) Alternator output (*I*t) Alternator or system voltage (*U*B+)
- Phase « Off »: Electric polarization Salt fog pulverization
- : +35°C, : 5%, : 0.1 Mpa, : 1.5 ml/h, : 6 000 min-1,
- : *I* /3 at 4 000 min-1/ +23°C, : *U*reg,
- : without, : without.
- Cycles Number: 77 (equivalent of 96 h), For liquid cooled alternator, no liquid flow & electrical output defined in order to have *T*j diode < *T*j maxi.

The motor with the MagDrive magnets in the test bench

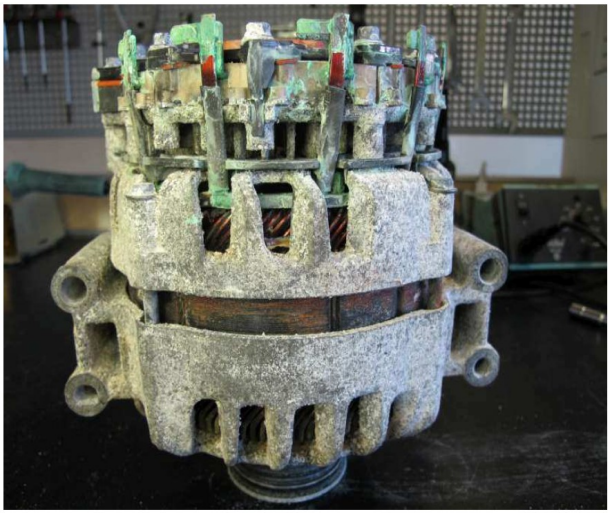

The rotor after the salt-spray test

The MagDrive magnets turned out to be suitable for the application, there was no magnet degradation, the test was passed successfully, and there were no performance losses.

The final tests were devoted to the evaluation of the performance of the electric-motor containing the MagDrive magnets. The measurements were carried out at different working temperature and rotation speeds. The most relevant output values were the torque and power, which were compared to the predictions of the simulations:

SIMULATION VALUE CAN ACQUISITION BENCH MEASURMENT

								CAN datas						Bench Measurements							Temperatures			
Speed (rpm)	Udc (V)	Idc (A)	Pelec *target* (W)	Id (CAN meas.) (A)	Iq (CAN meas.) (A)	Iabs (A)	Tamb (°C)	PWB OARD _T[°C]	CTRLB OARD _T[°C]	STAT OR_T [°C]	RO TO R_T	TORQ UE_E STIM ATED	EXC_ CUR RENT	Udc (V)	Idc	Pelec	Speed	Estimated Torque	Pmeca	Efficiency	module 2	2	Lead frame	3
70°C																								
1650	48	24,2	1162	0	-40		70	84	85	115	100	-12,8	2,9	48,0	24,2	1162	1650	-9,2	-1590	73%	103	106	106	87
1650	48	28,9	1387	0	-46		70	89	86	127	112	-15,0	3,3	48,0	29,0	1392	1650	-10,9	-1883	74%	111	114	115	92
1650	48	33,4	1603	0	-52		70	94	88	138	121	-17,0	3,6	48,0	33,4	1603	1650	-12,7	-2194	73%	119	123	124	97
1650	48	42,8	2054	0	-64	64	70	106	92	170	143	-21,0	4,3	48,0	42,9	2059	1650	-16,5	-2851	72%	140	146	148	109
2250	48	41,9	2011	0	-46	46	70	86	85	132	117	-15,0	3,3	48,0	41,9	2011	2250	-11,2	-2639	76%	106	109	110	92
2250	48	48,3	2318	0	-52	52	70	89	85	139	120	-16,8	3,6	48,0	48,5	2328	2250	-12,9	-3039	77%	112	116	117	95
2250	48	62,0	2976	0	-64	64	70	98	88	168	144	-20,0	4,3	48,0	62,0	2976	2250	-16,5	-3888	77%	129	135	136	107
3000	48	67,0	3216	0	-52	52	70	85	83	142	116	-17,0	3,6	48,0	67,0	3216	3000	-13,0	-4084	79%	107	110	111	94
3000	48	72,0	3456	0	-55	55	70	86	83	145	116	-18,0	3,8	48,0	72,0	3456	3000	-14,0	-4398	79%	109	113	114	95
3000	48	86,0	4128	0	-64	64	70	92	85	166	136	-21,0	4,3	48,0	86,2	4138	3000	-16,6	-5215	79%	119	124	126	103
100°C																								
1650	48	23,8	1142	0	-40		100	110	115	149	136	-13,0	2,9	48,0	23,8	1142	1650	-9,2	-1590	72%	135	138	139	118
1650	48	28,5	1368	0	-46	46	100	115	118	157	141	-15,0	3,3	48,0	28,6	1373	1650	-10,9	-1883	73%	143	147	148	122
2250	48	34,7	1666	0	-40	40	100	108	114	149	129	-13,0	3,0	48,0	34,6	1661	2250	-9,4	-2215	75%	131	134	135	117
2250	48	41,2	1978	0	-46	46	100	111	115	160	140	-15,0	3,3	48,0	41,3	1982	2250	-11,2	-2639	75%	138	142	143	121
2250	48	48,0	2304	0	-52	52	100	116	117	171	150	-16,5	3,6	48,0	48,0	2304	2250	-13,0	-3063	75%	145	150	151	126
3000	48	66,8	3206	0	-52	52	100	112	115	175	148	-17,0	3,7	48,0	66,8	3206	3000	-13,2	-4147	77%	140	145	146	125
3000	48	71,2	3418	0	-56	56	100	114	115	180	149	-18,0	3,8	48,0	71,2	3418	3000	-13,9	-4367	78%	143	148	149	127
4000	48	81,0	3888	-36	-53	64,1	100	112	114	184	155	-17,0	3,7	48,0	81,0	3888	4000	-12,2	-5110	76%	144	150	151	130
5000	48	109,7	5266	-35	-54	64,4	101	101	109	191	140	-17,0	3,7	48,0	109,7	5266	5000	-12,9	-6754	78%	120	120	122	114
6000	48	158,3	7598	-68	-58	89,4	101	100	108	190	132	-19,0	4,3	48,0	158,2	7594	6000	-14,9	-9362	81%	118	118	119	114
105°C																								
1650	48	24,1	1157	0	-40	40,0	105	116	122	155	142	-13,0	3,0	48,0	24,1	1157	1650	-9,1	-1572	74%	142	145	146	124
1650	48	28,8	1382	0	-46	46,0	105	120	124	166	150	-14,7	3,3	48,0	28,6	1373	1650	-10,9	-1883	73%	150	153	155	128
2250	48	34,6	1661	0	-40	40,0	105	113	120	161	148	-13,0	3,0	48,0	34,6	1661	2250	-9,4	-2215	75%	138	141	142	125
2250	48	41,1	1973	0	-46	46,0	105	116	121	168	150	-14,5	3,3	48,0	41,1	1973	2250	-11,0	-2592	76%	144	148	149	127
2250	48	47,6	2285	0	-52	52,0	105	120	123	179	159	-17,0	3,6	48,0	47,7	2290	2250	-12,9	-3039	75%	152	156	158	132
3000	48	66,4	3187	0	-52	52,0	105	116	120	181	155	-17,0	3,6	48,0	66,3	3182	3000	-13,0	-4084	78%	146	150	151	131
3000	48	71,0	3408	0	-56	56,0	105	118	120	185	155	-18,0	3,8	48,0	70,8	3398	3000	-13,9	-4367	78%	148	153	155	132
4000	48	76,0	3648	-33	-50	59,9	105	114	118	183	157	-16,0	3,5	48,0	76,0	3648	4000	-11,3	-4733	77%	144	150	151	133
5000	48	109,5	5256	-35	-54	64,4	105	106	115	198	146	-17,0	3,7	48,0	109,5	5256	5000	-12,8	-6702	78%	125	125	127	120
6000	48	158,5	7608	-68	-58	89,4	105	104	114	197	141	-19,6	4,3	48,0	158,6	7613	6000	-14,8	-9299	82%	123	123	125	121

The measured quantities were monitored during the tests:

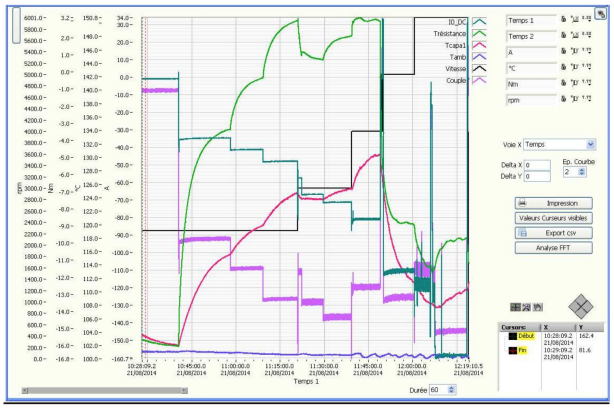

The rotor equipped with the MagDrive magnets fulfilled the specifications. There was no demagnetization, the correlation between the simulation and measured results was good, hence all the objectives were achieved. The conclusion was that the MagDrive magnets, with reduced amount of heavy rare-earth elements, can be used in electric motors.

9 WP 9: Dissemination and exploitation (M1 - M36)

WP Leader: Matej Komelj (JSI)

Summary of Results

Dissemination and exploitation of project results are very important aspects of all European projects. Dissemination in the MAG-DRIVE project was carried out in various forms, some of them are conference talks and posters, invited lectures as well as internal dissemination of various aspects of the projects, carried out by each of the partners. The outcome of the research activities within the project resulted in one patent application. We prepared a detailed exploitation plan for an eventual upscaling of the HDDR+SPS magnet production. The break-even point, at which the initial one-off investment costs equal the profit, would be expected to occur at the end of the third quarter of the third year after starting the production.

There are no deviations from the objectives and task given in Annex I.

Details for each Task

9.1 Task 9.1: Dissemination (M1 – M36)

During the entire course of the project the members of the MAG-DRIVE consortium disseminated the activities as well as results of the project. The dissemination activities included the creation of the project website as well as oral presentation at various conferences.

No.	Type of activities	Main leader	Title	Date	Place	Type of audience	Size of audience	Countries addressed
1	Oral presentation to a wider public	JSI	Examples of European projects relating to permanent-magnets with reduced quantities of, or zero, rare earths	27/08/13	JEMS 2013, Rhodes, Greece	Scientific community (higher education, Research)		International conference
2	Organisation of Workshops	JSI	First MAG-DRIVE workshop	06/03/14	JSI Department for Nanostructured Materials, Ljubljana, Slovenia	Scientific community (higher education, Research)-Industry		European countries
3	Web sites/Applications	JSI	MAG-DRIVE project website	06/03/14	http://mag-drive-fp7.eu/	Industry-Civil		International website

						society-Media	
4	Web sites/Applications	JSI	MAG-DRIVE facebook website	15/05/15	https://www.facebook.com/Mag-Drive-Project-346378675555086/	Civil society Media	International website
5	Oral presentation to a scientific event	JSI	The rapid densification of Nd-Fe-B materials using spark-plasma sintering	19/08/14	Annapolis, MA USA-REPM2014	Scientific community (higher education, Research)-Industry	International public
6	Oral presentation to a scientific event	JSI	MAG-DRIVE and EC-funded project to reduce the dependence of the European automotive industry on REEs	06/09/14	Milos Island, Greece	Scientific community (higher education, Research)	EU countries
7	Oral presentation to a scientific event	QMUL	Processing of magnetic materials by novel Flash Spark Plasma Sintering method	22/05/16	JSI, Ljubljana, Slovenia	Scientific community (higher education, Research)	EU countries
8	Oral presentation to a scientific event	QMUL	Spark Plasma Sintering of permanent magnets. Workshop in Innovative Materials for Ecologic Vehicles	18/11/15	Imev, Paris, France	Scientific community (higher education, Research)	EU countries
9	Oral presentation to a scientific event	QMUL	Keynote: Permanent	14/09/15	Institute IMDEA,	Scientific community	EU

			magnets for electric motors: requirements and challenges. Nanopyme Workshop "Rare Earth-Free Permanent Magnets and Applications"		Madrid, Spain	(higher education, Research)	countries
10	Oral presentation to a scientific event	QMUL	Spark Plasma Sintering of permanent magnetic materials for next-generation Electric Vehicle motors.	10/09/15	EUROCON 2015, Salamanca, Spain	Scientific community (higher education, Research)	International public
11	Oral presentation to a scientific event	ICTM	Surfactant-assisted high energy ball milling technique as a method for preparation of magnetic submicrometer particles	05/09/16	YUCOMAT 2016, Herceg Novi, Montenegro	Scientific community (higher education, Research)	International public
12	Oral presentation to a scientific event	ICTM	Characterization of NdFeB magnetic submicron particles obtained by surfactant-assisted high energy ball milling (SA-HEBM)	05/09/16	YUCOMAT 2016, Herceg Novi, Montenegro	Scientific community (higher education, Research)	International public

13	Oral presentation to a scientific event	ICTM	Modelling the magnetophoresis and gravity settling-based size separation of NdFeB magnetic microparticles	11/06/15	IcETRAN 2015, Srebrno Jezero, Serbia	Scientific community (higher education, Research)	Internatinal public
14	Posters	QMUL	Microstructural control of Nd-Fe-B materials sintered using electric Field Assisted Sintering Techniques (FAST)	-/07/15	ICM2015, Barcelona, Spain	Scientific community (higher education, Research)	International public
15	Posters	ICTM	Preparation of NdFeB magnetic nanoparticles by surfactant-assisted high energy ball milling	02/09/15	YUCOMAT 2015, Herceg Novi, Montenegro	Scientific community (higher education, Research)	International public
16	Posters	QMUL	Novel “Flash Spark Plasma Sintering” method for the rapid fabrication of nanostructured and anisotropic rare-earth lean permanent magnetic materials	28/08/16	REPM2016, Darmstadt, Germany	Scientific community (higher education, Research)	International public
17	Posters	JSI	Development of permanent magnets for electric vehicles	20/04/16	TRA2016, Warsaw, Poland	Scientific community (higher education, Research)	International public

18	Organization of Workshops	QMUL	MAG-DRIVE meeting & magnetic materials/SPS seminar	05/02/15	QMUL, London, UK	Scientific community (higher education, Research)	European countries
19	Organization of Workshops	Valeo	MAG-DRIVE meeting & magnets in automotive industry	18/09/15	Valeo, Paris, France	Scientific community (higher education, Research)	European countries
20	Organization of Workshops	ICTM	MAG-DRIVE meeting & mechanical milling techniques	22/04/16	ICTM,Belgrade, Serbia	Scientific community (higher education, Research)	European countries
21	Organization of Workshops	KE	MAG-DRIVE meeting&wire-explosion technique for massive production	22/09/16	KE, Neustadt, Germany	Scientific community (higher education, Research)	European countries
22	Peer-reviewed publication	UoB	The development of microstructure during hydrogenation–disproportionation–desorption–recombination treatment of sintered neodymium-iron-boron-type magnets	01/03/16	Journal of Magnetism and Magnetic Materials 401, 455-462	Scientific community (higher education, Research)	International public
23	Peer-reviewed publication	UoB	Rapid sintering of anisotropic, nanograined Nd–Fe–B by flash-spark plasma sintering	01/11/16	Journal of Magnetism and Magnetic Materials 417, 279-283	Scientific community (higher education, Research)	International public

As one can see the project was being presented at some of the major scientific conferences, such as REPM2014,REPM16, TRA2016, and the results were published in high-impact journals like Journal of Magnetism and Magnetic Materials.

9.2 Task 9.2: Exploitation (M1 - M36)

The development of an exploitation plan as foreseen in the DoW began in the second half of the project.

Harmonization with the MAG-DRIVE Consortium Agreement / Grant Agreement, especially for publications and IPR was achieved beforehand. Before the midterm meeting in London it was decided that all material meant for publishing needed to be evaluated by all of the partners prior to their submission.

As part of exploitation activities we also contacted our advisory board members for help with topics pertaining to this project. From such collaboration with Dr. David Brown we managed to acquire samples, which were vital for the scientific development in WP 3.

The research outcome resulted in the patent application: Flash Spark Plasma Sintering of fully dense, nanostructured permanent magnetic materials - Elinor G. Castle, Richard Sheridan, Salvatore Grasso, Allan Walton, Mike Reece - Patent application No. GB1600587.8 - 12th Jan 2016

All three routes, developed in the work-packages WP3, WP4 and WP5 proved to be potentially interesting for scaling up to the commercial level. However, it was decided that the HDDR+SPS route in WP5 contained most elements, relatively easily transferable from a lab to an industrial level. Therefore, a detailed exploitation plan was prepared by having in mind this sort of production.

The massive production would require a purchase of a new, customized, multi-chamber SPS equipment, which costs about € 1.74M. For the FSPS process suggested, an additional chamber for the hopper loading and cold pressing of the Nd-Fe-B powder would have to be developed and added to the machine; at an estimated maximum cost of € 580k. The investment required for the research and development of the custom machine would be roughly € 232k. With attendant costs of building, services and other incidental one-off expenses, the total one-off cost for the customised SPS machine and installation is expected to be around € 2.9M:

Investment	**Estimated Cost (€)**
Machine research and development investment	€231 k
New multi-chamber SPS furnace and associated equipment, in accordance with FSPS requirements and desired throughput	€2.3 M
Building / Services to accommodate new SPS facility	€578 k
Purchase of handling aids to help in periodic removal of large numbers of magnets from the machine and to refill the hopper with powder.	€34.6 k
Total (max)	**€3.16 M**

Ongoing running costs associated with the SPS include:

Part of the time of a trained technician to periodically load the hopper with powder and remove cooled magnets from the machine. Considering two technicians working back-to-back for overnight production, this could equate to a pro rata cost of € 35 k per annum.

Replacement of custom made FSPS graphite tooling and purchase of different sets for different desired magnet shapes. For the proposed net shape FSPS process this only relates to the punches being used. Given the relatively low pressures required for the small magnets the punches are expected to last for up to 200 runs. It is therefore recommended that the punches be changed twice a day. Considering the highest output case of the multi-processing of 10 magnets at once, this equates to 100 punch sets a week and 5200 punch sets in a year. The cost for one set of custom designed punches is € 58, hence this is an ongoing expense of € 302,000 per year. Potential savings could be made by producing the punch sets in-house.

Ongoing SPS maintenance and repairs, € 23-35k per year.

Energy bills for running of the SPS machine. The FSPS process consumes around 0.02 kWh per magnet, which at a maximum throughput of 7200 magnets per day, would equate to 144 kWh per day or 37,440 kWh per annum. Factoring in other associated energy costs (e.g. the intermittent running of a vacuum pump and chiller), the annual energy consumption is expected to be roughly 70,000 kWh/annum; costing around € 8k

Investment	**Estimated cost per year (€)**
Technician time	€34.7 k
Graphite tooling	€300.5 k
SPS maintenance and repairs	€23-34.7 k
Energy bills	€8.1 k
Total (max)	**€377.9 k**

The current cost to make and ship a standard 12g Nd-Fe-B magnet containing 10 wt.% Dy is around € 1.2. This price is based on analysis of the current Chinese local market and cost when supplied to Europe, as determined in consultation with Valeo. Of this figure, the raw materials cost accounts for €1.056.

For a Dy-free composition, as per the current MQU-F material being processed by FSPS, the raw materials cost would be €0.4 per magnet. For a maximum output of 7200 magnets per day, this equates to an **annual raw materials cost of around €760,000**.

Taking into account the ongoing and raw materials costs, and neglecting the initial one-off costs, **the cost of production per magnet equals €0.608.** If the magnets were retailed at a competitive market price of €1.20 each plus VAT, this would equate to a profit of €0.592 per magnet and €1,108,224 per annum.

The break-even point, at which the initial one-off investment costs equal the profit, would therefore be expected to occur at the end of the third quarter of the third year.

10 Project management during the period

The MAG-DRIVE management was lead by JSI. The main goals were to:

- Ensure efficient project coordination, progress monitoring, budget and financial control
- Ensure the quality of all activities and the timely delivery of reports and deliverables
- Ensure effective and on-time communication between the project consortium and the European Commission through the REA
- Prepare the rolling 6-monthly Action Plan

The coordinator was responsible for the day-to-day coordination of the project, project planning, progress, reports, deliverables, cost statements and budgetary overviews, contract negotiations and all financial and legal , issues, contingency plans and risk management, notes, minutes, and other materials, managing any necessary changes to plans or contracts, ensuring that the project proceeds on time and on budget , and represented the interface between the consortium and the REA. JSI prepared the Consortium Agreement, which was approved by all partners.

A rolling Action Plan was prepared every six months. It included details about the activities for the next six months, broken down to a weekly schedule of sample movements, tests, results, and information flow between partners.

The MAG-DRIVE website with the url address http://mag-drive-fp7.eu was created. The website features a public-accessibly area and an intranet section. The intranet section can be left via a logout function, for safety reasons. The website was regularly maintained and frequently updated.

List of project meetings, dates, venues

11.10. 2013 *Brussels*
First meeting (11 participants)

04. 04. 2014 *Brussels*
M6 meeting (11 participants)

17. 10. 2014 *Brussels*
M12 meeting (14 participants)

05. 02. 2015 *London*
M18 meeting (15 participants)

17.09. 2015 *Paris*
M24 meeting (14 participants)

21.04. 2016 *Belgrade*
M30 meeting (15 participants)

21.09. 2016 *Neustadt*
M36 meeting (13 participants)

From all meetings, agendas, presentations, minutes and photos are available for download on the protected part of the MAG-DRIVE web page.

Amendment to the grant agreement

On 04. 02. 2015 an amendment to the grant agreement was issued. It specifies the change of the name and address of the project coordinator in Article 8.1 of the grant agreement as:

Dr. Matej Komelj

INSTITUT JOZEF STEFAN

Department of Nanostructured materials

Jamova 39

LJUBLJANA 1000

SLOVENIA

and in Article 8.3 as: matej.komelj@ijs.si

Accordingly also the Part A and B of the Annex I were modified. The valid version is dated 19. 01. 2015

Deviations from the planned deliverables

On the basis of the first research activities within WP3 it was decided that the nature of the deliverables D3.1 D3.2 and D3.3 was changed from the prototype to the report. For the same reason the deliverable D3.4 was postponed from M18 to M24. All the changes were approved by the project officer, and they did not have any impact on the realization of the project objectives.

Communication with the External advisory board

Dr. David Brown, a member of the External advisory board, was contacted monthly for advices related to activities within WP3.

Deliverables and milestones tables

1 Deliverables

No.	Deliverable title	Ver.	WP no.	Lead benef.	Nature	Diss. level	Delivery date from Annex I (project month)	Actual delivery date (dd/mm/yy)	Status	Commen.
D1.1	Project website		1	JSI	O	PU	M12	04/05/15	Accepted	
D1.2	Project website		1	JSI	O	PU	M24	11/11/16	Received	
D1.3	Project website		1	JSI	O	PU	M36	11/11/16	Received	
D2.1	Survey of motors for pure Evs and hybrid Evs plus power electronics		2	VALEO	R	PP	M3	24/02/14	Accepted	
D2.2	Survey of magnetic materials and technologies		2	JSI	R	PP	M3	21/02/14	Accepted	
D2.3	Technical specifications for power electronics		2	VALEO	R	PP	M8	22/09/14	Accepted	

No.	Deliverable title	Ver.	WP no.	Lead benef.	Nature	Diss. level	Delivery date from Annex I (project month)	Actual delivery date (dd/mm/yy)	Status	Commen.
D2.4	Technical specifications for magnets	2	JSI	R	PP	M8	22/09/14	Accepted		
D3.1	Test cores of simple geometry made from $Nd_2Fe_{14}B$	3	KE	R	PP	M12	04/05/15	Received		changed from P to R
D3.2	Test cores of simple geometry made from Sm_2Co_{17}	3	KE	R	PP	M12	04/05/15	Received		changed from P to R
D3.3	Hard magnetic materials made from super-structured co-precipitated oxides of Nd, FeB	3	KE	R	PP	M15	05/05/15	Received		changed from P to R
D3.4	Hard magnetic material made from super-structured co-precipitated oxides of Sm_2Co	3	KE	P	PP	M24	03/12/15	Received		postponed from M18 to M24
D3.5	Report detailing parts of complex 3D-shape for industrial use in EV made along the Kochanek process from materials of either D3.1 or D3.2	3	JSI	R	PP	M30	15/11/16	Received		
D3.6	To develop a physical theory that allows to understand the magnetic properties in super-structured magnetic materials made along the Kochanek process	3	4	UoB	R	PU	M30	12/05/16	Received	
D4.1	Survey of nano-milling technologies and	4	6	ICMT	R	PP	M6	26/03/14	Accepted	

No.	Deliverable title	Ver.	WP no.	Lead benef.	Nature	Diss. level	Delivery date from Annex I (project month)	Actual delivery date (dd/mm/yy)	Status	Commen.
	characteristics									
D4.2	Micrometer particles of 3-5 µm		4	ICMT	P	PP	M12	04/05/15	Accepted	
D4.3	Sub-micrometer particles of less than 1 µm produced		4	ICMT	P	PP	M20	20/07/15	Accepted	
D4.4	Developed technologies for the separation of nanoparticles		4	ICMT	P	PP	M24	30/11/15	Received	
D4.5	Nd-Fe-B permanent magnets for EV applications		4	ICMT	R	PP	M30	15/11/16	Received	
D5.1	Optimised HDDR processing conditions for a variety of input materials		5	UoB	P	PP	M9	22/09/14	Accepted	
D5.2	Optimised HDDR processing conditions for variety of input materials		5	UoB	P	PP	M15	04/05/15	Received	
D5.3	Successful production of aligned dense compacts suitable for SPS		5	UoB	P	PP	M18	04/05/15	Received	
D5.4	Report on densification kinetics and model of the process		5	UoB	R	PP	M18	06/05/15	Received	
D5.5	Report on densification kinetics and model of the process		5	UoB	R	PP	M24	30/11/15	Received	
D5.6	Report detailling fully		5	QMUL	R	PP	M30	12/05/15	Received	

No.	Deliverable title	Ver.	WP no.	Lead benef.	Nature	Diss. level	Delivery date from Annex I (project month)	Actual delivery date (dd/mm/yy)	Status	Commen.
	dense alligned Nd-Fe-B magnets suitable for EV applications									
D6.1	Scanning electron microscopy reports detailing activities for the project		6	JSI	R	PP	M12	04/05/15	Accepted	
D6.2	Advanced electron microscopy reports detailing activities for the project		6	UoB	R	PP	M12	04/05/15	Accepted	
D6.3	Magnetic measurements reports detailing activities for the project		6	JSI	R	PP	M12	04/05/15	Accepted	
D6.4	Scanning electron microscopy reports detailing activities for the project		6	JSI	R	PP	M18	11/05/15	Accepted	
D6.5	Advanced electron microscopy reports detailing activities for the project		6	UoB	R	PP	M18	19/05/15	Accepted	
D6.6	Magnetic measurements reports detailing activities for the project		6	JSI	R	PP	M18	15/05/15	Accepted	
D6.7	Surface properties and particle size reports		6	ICTM	R	PP	M18	06/05/15	Accepted	
D6.8	Corrosion tests reports detailing activities for the project		6	VALEO	R	PP	M18	04/05/15	Accepted	
D6.9	Scanning electron microscopy reports		6	JSI	R	PP	M24	22/02/16	Received	

No.	Deliverable title	Ver.	WP no.	Lead benef.	Nature	Diss. level	Delivery date from Annex I (project month)	Actual delivery date (dd/mm/yy)	Status	Commen.
	detailing activities for the project									
D6.10	Advanced electron microscopy reports detailing activities for the project		6	JSI	R	PP	M24	03/12/15	Received	
D6.11	Magnetic measurements reports detailing activities for the project		6	JSI	R	PP	M24	12/01/16	Received	
D6.12	Surface properties and particle size reports		6	ICTM	R	PP	M24	30/11/15	Received	
D6.13	Corrosion tests reports detailing activities for the project		6	VALEO	R	PP	M24	22/07/16	Received	
D6.14	Surface properties and particle size reports		6	ICTM	R	PP	M30	19/07/16	Received	
D6.15	Scanning electron microscopy reports detailing activities for the project		6	JSI	R	PP	M35	11/11/16	Received	
D6.16	Advanced electron microscopy reports detailing activities for the project		6	JSI	R	PP	M35	15/09/16	Received	
D6.17	Magnetic measurements reports detailing activities for the project		6	JSI	R	PP	M35	11/11/16	Received	
D6.18	Corrosion tests reports detailing activities for the project		6	VALEO	R	PP	M35	15/11/16	Received	
D7.1	Report on equipment		7	MAGNETI	R	PP	M20	04/08/15	Accepted	

No.	Deliverable title	Ver.	WP no.	Lead benef.	Nature	Diss. level	Delivery date from Annex I (project month)	Actual delivery date (dd/mm/yy)	Status	Commen.
	producing new magnets									
D7.2	Report on pressing, characterisation and sintering		7	MAGNETI	R	PP	M24	25/12/15	Received	
D7.3	Permanent magnets delivered		7	VALEO	R	PP	M26	11/11/16	Received	
D7.4	Power electronics investigated, optimised and delivered		7	VALEO	D	PP	M28	14/11/16	Received	
D7.5	Electrical motors and permanent magnets are integrated and the whole EM is ready for testing		7	VALEO	D	PP	M30	14/11/16	Received	
D8.1	Testing procedure defined		8	VALEO	R	PP	M26	15/11/16	Received	
D8.2	Report on magnetic and physical properties		8	MAGNETI	R	PP	M28	16/11/16	Received	
D8.3	Report on corrosion tests		8	VALEO	R	PP	M28	15/11/16	Received	
D8.4	Report on the completed testing procedure		8	VALEO	R	PP	M34	15/11/16	Received	
D8.5	MAG-DRIVE meeting, evaluation and future directions		8	JSI	O	PP	M35	14/11/16	Received	
D9.1	Dissemination mid-project report		8	JSI	R	PU	M18	06/05/15	Accepted	
D9.2	Exploitation mid-project report		8	JSI	R	PP	M18	08/05/15	Accepted	

No.	Deliverable title	Ver.	WP no.	Lead benef.	Nature	Diss. level	Delivery date from Annex I (project month)	Actual delivery date (dd/mm/yy)	Status	Commen.
D9.3	Exploitation Plan		8	JSI	R	PP	M30	12/11/16	Submitted	
D9.4	Final Report		8	JSI	R	PP	M36		Pending	Recent document

Conclusions regarding deliverables

D3.1 - Test cores of simple geometry made from $Nd_2Fe_{14}B$
decided and approved by the project officer to change the nature from “prototype” to “report”

D3.2 - Test cores of simple geometry made from Sm_2Co_{17}
decided and approved by the project officer to change the nature from “prototype” to “report”

D3.3 - Hard magnetic materials made from super-structured co-precipitated oxides of Nd, FeB
decided and approved by the project officer to change the nature from “prototype” to “report”

D3.4 - Hard magnetic material made from super-structured co-precipitated oxides of Sm_2Co
decided and approved by the project officer to postpone the deliverable from M18 to M24

2 Milestones

Milestone no.	Milestone name	Workpackage no.	Lead. Beneficiary	Delivery date from Annex I dd/mm/yyyy	Achieved Yes/No	Actual/Forecast achievement date dd/mm/yyyy	Comments
MS1	Technical Specification For New Magnets Defined	WP2	VALEO	31/05/2014	Yes	22/09/14	we specified the size and shape, magnetic, mechanical and corrosion-resistance properties
MS2	Midterm Review	WP1	JSI	31/03/2015	Yes	29/05/15	the document was submitted
MS3	First Demonstrators Assembled	WP7	MAGNETI	31/08/2015	Yes	17/09/15	It was reported about the first sintered magnets during the meeting in Paris
MS4	Project Finished	All	JSI	31/09/2016	Yes		all goals were achieved and all reports, including the present document, were delivered on time